HIGH TEMPERATURE CORROSION OF SINGLE CRYSTAL SAPPHIRE AND ZIRCONIA IN COAL GASIFICATION AND COMMERCIAL GLASS ENVIRONMENTS

Zorana Dicic

Thesis submitted to the Faculty of the Virginia Polytechnic Institute and State University in partial fulfillment of the Requirements for the degree of

Master of Science
In
Materials Science and Engineering

APPROVED:

_____	_____
Dr. Anbo Wang, co-Chair	Dr. Gary Pickrell, co-Chair

_____
Dr. Steve Kampe

May 22, 2004
Blacksburg, Virginia

Keywords:
sapphire, alumina, coal slag, soda lime glass, coal gasifier, coal gasification, corrosion, corrosion rate, reaction kinetics.

HIGH TEMPERATURE CORROSION OF SINGLE CRYSTAL SAPPHIRE AND ZIRCONIA IN COAL GASIFICATION AND COMMERCIAL GLASS ENVIRONMENTS

By Zorana Dicic

Abstract

To meet the requirements of precise temperature monitoring at high temperatures in extremely corrosive environments, such as in coal gasifiers, a new sensor technology has been developed. This optical, ultra high temperature measurement system utilizes single crystal sapphire as a sensing element. A series of experiments was performed to determine the corrosion resistance of single crystal sapphire and single crystal fully stabilized cubic zirconia at high temperatures in coal slag and soda lime glass. The amount of corrosion of sapphire and zirconia in corrosive slags was measured at 1200^{o}C, 1300^{o}C, and 1400^{o}C for different exposure times. The microstructural features at the interface of sapphire and zirconia were investigated using SEM and EDX analysis. The experimental measurements as well as SEM micrographs show very little or no degradation of sapphire and zirconia samples in corrosive slags. An interesting phenomenon was observed in the EDX scans of sapphire in the coal slag: the iron from the slag appears to have completely separated from the silicon and deposited at the sapphire surface. This interesting observation can be further explored to study whether this iron layer can be used to control the corrosion of sapphire.

Acknowledgements

I would like to thank the Materials Science Department at Virginia Tech for accepting me into their program and giving me the opportunity to attain an M.S degree in this field. I am greatly thankful to my co-advisors, Dr. Gary Pickrell and Dr. Anbo Wang, for making me a part of their research team.

Table of Contents

ABSTRACT ..... **II**

ACKNOWLEDGEMENTS ..... **III**

TABLE OF CONTENTS ..... **IV**

LIST OF FIGURES ..... **V**

LIST OF TABLES ..... **IX**

1. INTRODUCTION **1**

2. LITERATURE REVIEW **8**

2.1 SAPPHIRE 8

2.1.1 Corrosion of sapphire *9*

2.1.2 Sapphire in silica melts *10*

2.1.3 Sapphire in Coal Slag *12*

2.2 ZIRCONIA 13

2.2.1 Corrosion of zirconia in different slags *16*

3. EXPERIMENTAL PROCEDURE **19**

3.1 MATERIALS SELECTION 19

3.2 COAL SLAG 21

3.3 SODA LIME GLASS 22

3.4 SAMPLE PREPARATION 22

3.5 HEAT TREATMENT 23

3.6 THICKNESS MEASUREMENTS 26

3.6.1 HF Method *27*

3.6.2 SEM Method *29*

3.7 COMPLEXITY OF HIGH TEMPERATURE CORROSION EXPERIMENTS 29

4. RESULTS AND DISCUSSION **31**

4.1 SAPPHIRE 31

4.1.1. Sapphire in Coal Slag *31*

4.1.1.1 Thickness Data 31

4.1.1.2 Surface and interface analysis 34
4.1.2. Sapphire in Soda Lime 44
4.1.2.1 Thickness Data 44
4.1.2.2 Surface and interface analysis 45
4.2 ZIRCONIA 55
4.2.1. Zirconia in Coal Slag 56
4.2.1.1 Thickness Data 56
4.2.1.2 Surface and interface analysis 57
4.2.2. Zirconia in Soda Lime Glass Slag 64
4.2.2.1 Thickness Data 64
4.2.2.2 Surface and interface analysis 65
4.3 ACTIVATION ENERGIES 74
4.4 ERROR ANALYSIS 75
4.4.1. Difficulties with HF Treatment 75
4.4.2 SEM Method Induced Errors 77
4.4.3 Sources of Errors due to Experimental Methods 78
4.4.4 Zirconia cracking 83
5. SUMMARY AND CONCLUSIONS 84
6. FUTURE WORK 86
REFERENCES 87
VITA 89

List of Figures

FIGURE 1-1- DIAGRAM OF COAL GASIFIER AND ALL OF ITS PRODUCTS 4
FIGURE 1-2- SCHEMATIC DESIGN OF BPDI TECHNOLOGY BASED OPTICAL HIGH TEMPERATURE MEASUREMENT SYSTEM 7
FIGURE 2-1- PHASE DIAGRAM OF YTTRIA-ZIRCONIA SYSTEM 14
FIGURE 2-2- PLOT OF THERMAL CONDUCTIVITY VS. THERMAL EXPANSION COEFFICIENT. YSZ HAS A 16
FIGURE 3-1- COMPOSITION OF COAL SLAG 21
FIGURE 3-2- COMPOSITION OF SODA LIME GLASS 22
FIGURE 3-3- DIAMOND SAW 23
FIGURE 3-4- SAMPLES OF SAPPHIRE AND ZIRCONIA IN: (A) EMPTY ALUMINA CRUCIBLE, (B) COAL SLAG AND (C) SODA LIME GLASS 24
FIGURE 3-5- FURNACE 25
FIGURE 3-6- SAMPLE OF SAPPHIRE IN COAL SLAG AFTER THE HEAT TREATMENT 26
FIGURE 3-7- CROSS SECTIONAL CUT OF SAPPHIRE IN COAL SLAG 26
FIGURE 3-8- CROSS SECTIONAL CUT OF SAPPHIRE AND ZIRCONIA IN SODA LIME GLASS 27
FIGURE 4-1- CHANGE IN THICKNESS VERSUS REACTION TIME AND TEMPERATURE FOR SINGLE CRYSTAL SAPPHIRE IN COAL SLAG 34
FIGURE 4-2- SEM MICROGRAPH OF SAPPHIRE CORRODE IN COAL SLAG AT 1200^{o}C FOR 1 DAY 35
FIGURE 4-3- EDX SCAN OF SAPPHIRE- COAL SLAG INTERFACE AFTER CORROSION AT 1200^{o}C FOR 1 DAY (LEFT: SAPPHIRE, RIGHT: COAL SLAG) 36
FIGURE 4-4- EDX SCAN OF SAPPHIRE- COAL SLAG INTERFACE AFTER CORROSION AT 1200^{o}C FOR 2 DAYS (LEFT: COAL SLAG, RIGHT: SAPPHIRE) 37
FIGURE 4-5- SEM MICROGRAPH OF SAPPHIRE CORRODE IN COAL SLAG AT 1200^{o}C FOR 3 DAYS 38
FIGURE 4-6- SEM MICROGRAPH OF SAPPHIRE CORRODE IN COAL SLAG AT 1200^{o}C FOR 4 DAYS 39
FIGURE 4-7- SEM MICROGRAPH OF SAPPHIRE CORRODE IN COAL SLAG AT 1300^{o}C FOR 2 40
FIGURE 4-8- SEM MICROGRAPH OF SAPPHIRE CORRODE IN COAL SLAG AT 1300^{o}C FOR 3 DAYS 41
FIGURE 4-9- SEM MICROGRAPH OF SAPPHIRE CORRODE IN COAL SLAG AT 1300^{o}C FOR 3 DAYS 42
FIGURE 4-10- EDX SCAN OF SAPPHIRE- COAL SLAG INTERFACE AFTER CORROSION AT 1300^{o}C FOR 4 DAYS (LEFT: SAPPHIRE, RIGHT: COAL SLAG) 43
FIGURE 4-11- SEM MICROGRAPH OF SAPPHIRE CORRODED IN COAL SLAG AT 1400^{o}C FOR 4 DAYS 43
FIGURE 4-12- AMOUNT OF CORROSION VERSUS REACTION TIME AND TEMPERATURE FOR SINGLE CRYSTAL SAPPHIRE IN SODA LIME GLASS 45
FIGURE 4-13- SEM MICROGRAPH OF SAPPHIRE CORRODE IN SODA LIME GLASS AT 1200^{o}C FOR 1 DAY 46

FIGURE 4-14- SEM MICROGRAPH OF SAPPHIRE CORRODE IN SODA LIME GLASS AT 1200°C FOR 2 DAYS..... 46
FIGURE 4-15- SEM MICROGRAPH OF SAPPHIRE CORRODE IN SODA LIME GLASS AT 1200°C FOR 3 DAYS..... 47
FIGURE 4-16- SEM MICROGRAPH OF SAPPHIRE CORRODE IN SODA LIME GLASS AT 1200°C FOR 4 DAYS..... 48
FIGURE 4-17- SEM MICROGRAPH OF SAPPHIRE CORRODE IN SODA LIME GLASS AT 1300°C FOR 1 DAY..... 49
FIGURE 4-18- EDX SCAN OF SAPPHIRE- SODA LIME GLASS INTERFACE AFTER CORROSION AT 1300°C FOR 1 DAY (TOP: SAPPHIRE, BOTTOM: SODA LIME GLASS)..... 49
FIGURE 4-19- SEM MICROGRAPH OF SAPPHIRE CORRODE IN SODA LIME GLASS AT 1300°C FOR 2 DAYS..... 50
FIGURE 4-20- SEM MICROGRAPH OF SAPPHIRE CORRODE IN SODA LIME GLASS AT 1300°C FOR 3 DAYS..... 51
FIGURE 4-21- ELEMENTAL SCAN A SPOT ON SODA LIME GLASS NEXT TO THE INTERFACE WITH SAPPHIRE..... 52
FIGURE 4-22- ELEMENTAL SCAN OF A STOP ON THE SAPPHIRE- SODA LIME INTERFACE..... 53
FIGURE 4-23- ELEMENTAL SCAN OF A SPOT INSIDE THE SAPPHIRE..... 54
FIGURE 4-24- SEM MICROGRAPH OF SAPPHIRE CORRODE IN SODA LIME GLASS AT 1300°C FOR 4 DAYS..... 55
FIGURE 4-25- SEM MICROGRAPH OF ZIRCONIA CORRODED IN COAL SLAG AT 1200°C FOR 1 DAY..... 57
FIGURE 4-26- EDX SCAN OF ZIRCONIA- COAL SLAG INTERFACE AFTER CORROSION AT 1200°C FOR 1 DAY (LEFT: ZIRCONIA, RIGHT: COAL SLAG)..... 58
FIGURE 4-27- SEM MICROGRAPH OF ZIRCONIA CORRODED IN COAL SLAG AT 1200°C FOR 2 DAYS..... 59
FIGURE 4-28- SPOT SCAN ELEMENTAL ANALYSIS OF THE INTERFACE BETWEEN ZIRCONIA AND COAL SLAG AFTER 2 DAYS OF HEAT TREATMENT AT 1200°C..... 60
FIGURE 4-29- SPOT SCAN ELEMENTAL ANALYSIS OF ZIRCONIA'S SIDE OF THE INTERFACE WITH COAL SLAG AFTER 2 DAYS OF HEAT TREATMENT AT 1200°C..... 61
FIGURE 4-30- SEM MICROGRAPH OF ZIRCONIA CORRODED IN COAL SLAG AT 1300°C FOR 1 DAY..... 62
FIGURE 4-31- SEM MICROGRAPH OF ZIRCONIA CORRODED IN COAL SLAG AT 1300°C FOR 2 DAYS..... 63
FIGURE 4-32- SEM MICROGRAPH OF ZIRCONIA CORRODED IN COAL SLAG AT 1300°C FOR 3 DAYS..... 63
FIGURE 4-33- SEM MICROGRAPH OF ZIRCONIA CORRODED IN COAL SLAG AT 1300°C FOR 4 DAYS..... 64
FIGURE 4-34- SEM MICROGRAPH OF ZIRCONIA CORRODED IN SODA LIME GLASS AT 1200°C FOR 1 DAY..... 66
FIGURE 4-35- SEM MICROGRAPH OF ZIRCONIA CORRODED IN SODA LIME GLASS AT 1200°C FOR 2 DAYS..... 66
FIGURE 4-36- SEM MICROGRAPH OF ZIRCONIA CORRODED IN SODA LIME GLASS AT 1200°C FOR 3 DAYS..... 67
FIGURE 4-37- SEM MICROGRAPH OF ZIRCONIA CORRODED IN SODA LIME GLASS AT 1200°C FOR 4 DAYS..... 67
FIGURE 4-38- SEM MICROGRAPH OF ZIRCONIA CORRODED IN SODA LIME GLASS AT 1300°C FOR 1 DAY..... 68
FIGURE 4-39- SEM MICROGRAPH OF ZIRCONIA CORRODED IN SODA LIME GLASS AT 1300°C FOR 2 DAYS..... 69
FIGURE 4-40- SEM MICROGRAPH OF ZIRCONIA CORRODED IN SODA LIME GLASS AT 1300°C FOR 3 DAYS..... 69
FIGURE 4-41- ELEMENTAL SCAN OF THE SPOT ON SODA LIME GLASS NEXT TO THE INTERFACE WITH ZIRCONIA..... 70
FIGURE 4-42- ELEMENTAL SCAN OF THE SPOT ON ZIRCONIA NEXT TO THE INTERFACE WITH SODA LIME GLASS..... 71
FIGURE 4-43- ELEMENTAL SCAN OF THE SPOT ON ZIRCONIA SAMPLE..... 72

FIGURE 4-44- EDX SCAN OF ZIRCONIA- SODA LIME GLASS INTERFACE AFTER CORROSION AT 1300°C FOR 3 DAYS (LEFT: SODA LIME, RIGHT: ZIRCONIA) 73
FIGURE 4-45- SEM MICROGRAPH OF ZIRCONIA CORRODED IN SODA LIME GLASS AT 1300°C FOR 4 DAYS 73
FIGURE 4-46-SCHEMATIC REPRESENTATION OF THE ANGLE AT WHICH THE SAMPLE IS TILTED AND THEN SLICED INSIDE THE CRUCIBLE 78
FIGURE 4-47- SAPPHIRE IN COAL SLAG AT 1400°C FOR 4 DAYS IN 50ML CRUCIBLE 81
FIGURE 4-48- CORROSION OF SAPPHIRE IN COAL SLAG AT 1300°C 82
FIGURE 4-49- CORROSION OF SAPPHIRE IN COAL SLAG AT 1200°C 82
FIGURE 4-50- STRUCTURES OF THE THREE ZRO2 PHASES. THE ZR-O BONDS ARE ONLY SHOWN IN THE MONOCLINIC STRUCTURE. FOR THE TETRAGONAL PHASE, THE ARROWS INDICATE THE DISTORTION OF OXYGEN PAIRS RELATIVE TO THE CUBIC STRUCTURE. 83

List of Tables

TABLE 3-1- TABLE OF MATERIALS 20
TABLE 3-2- TABLE OF EQUIPMENT 20
TABLE 4-1- CHANGE IN THICKNESS OF SAPPHIRE IN COAL SLAG 33
TABLE 4-2- CHANGE IN THICKNESS OF SAPPHIRE IN SODA LIME GLASS 44
TABLE 4-3- CHANGE IN THICKNESS OF ZIRCONIA IN SODA LIME GLASS 57
TABLE 4-4- CHANGE IN THICKNESS OF ZIRCONIA IN SODA LIME SLAG 65
TABLE 4-5- CORROSION MEASUREMENTS OF SAPPHIRE IN COAL SLAG AT 1200^{O}C AND 1300^{O}C 81

1. INTRODUCTION

Today's industry is increasing the demand for materials with good performance in harsh environments under the conditions of extreme corrosion under high temperature and pressure.

Corrosion is one of the restricting factors for applications of ceramics in industry. Understanding the corrosion processes including the diffusion mechanisms that take place in ceramic materials in various environments can significantly improve current uses and give rise to new ones. Considerable research has been performed in the area of corrosion of materials to find suitable materials for coal gasification, coal liquification, energy storage, gas turbine power generation, fossil fuel processing and many other energy systems.

The extent of corrosion for a given material is very much dependant on the structure of the material- crystal size and shape, porosity and impurities present at the grain boundaries, which are common in structural ceramic materials. Along pores and grain boundaries are usually the most susceptible places for slag attack. To minimize corrosion, these structural factors should be eliminated. This can be accomplished by using a dense single crystal.

Corrosion processes in ceramics can be quite complex and vary greatly with the physical and chemical properties of the material and the environment to which they are subjected. In the slag corrosion process, physical factors such as thermal expansion mismatch between the slag and the ceramic phases, elastic and plastic deformation, velocity of the slag flow, and diffusion to or

away from the reaction interface must be considered. Similarly, chemical factors such as chemical composition of the slag and solubility of the ceramic material in that slag are vital for understanding the interfacial reactions during the corrosion. Understanding of the physical and chemical properties of a ceramic and a slag system can be utilized to yield higher corrosion resistance and therefore better performance and prolonged life in the industrial applications.

Even though corrosion of alumina and zirconia ceramics has been investigated in the past, the amount of available data is limited for single crystal sapphire and zirconia in coal slags. More information is necessary in order to complete the understanding of the corrosion processes and corrosion mechanisms in order to be able to predict the suitability of these materials for use in optical measurements inside coal gasification systems.

When corrosion of a solid in a liquid occurs, both thermodynamic and kinetic considerations have to be taken into account. Corrosion processes may proceed in stages. The particular stages depend on the type of material and the environment. During corrosion, several different processes proceed at the same time, for example transport of matter or energy to and from the interface and the reaction at the interface. There are many possible rate-controlling steps in the corrosion process. Some of the possible rate-controlling mechanisms include:

- Rate of the interfacial reaction at the interface between the solid sample and the corroding slag to form the reaction products;
- Dissolution rate of material dissolved in the slag;
- Mass transport or diffusion of species toward the interface;

- Mass transport or diffusion of species away from the interface.

For predictive capability, it is important to determine the rate-controlling step. In stationary specimens or unstirred liquids, the rate of dissolution of the solid into the liquid medium is governed by molecular diffusion away from the interface where the reaction takes place. High viscosity liquids typically result in very slow diffusion, and a thick boundary layer. Since the diffusion rate is much slower in viscous liquids, corrosion will more likely be controlled by material transport than by the interface reaction. However, this is not always the case.

This research project has been focused on understanding the reactions between coal slag from a coal gasification unit and single crystal sapphire and zirconia. In addition, reactions between borosilicate and soda lime glasses from commercial glass manufacturing operations and single crystal sapphire and single crystal zirconia were also investigated. Coal gasification is a clean and efficient way to produce electricity and hydrogen gas[1]. The amount of air or oxygen in the gasifier (Figure 1-1) is controlled in order to achieve only partial oxidation of the fuel. As a consequence of being exposed to hot steam and oxygen under high temperature and pressure, carbon containing feedstock is reacted to produce high, medium or low BTU fuel or to produce chemicals and process gases. In this process, carbon molecules break apart from coal and undergo chemical reactions to form a mixture of gases such as hydrogen, carbon monoxide, and others, also known as syngas. This process has the potential to produce clean-burning hydrogen for power-generating fuel cells, and carbon monoxide for fuel or chemical process feedstock. Coal gasification rather than coal combustion leads to cleaner and more efficient power generation processes, although many problems are encountered due to the corrosive nature of the constituents in the coal. Figure 1-1 shows a typical

combined cycle coal gasification/power generation facility. The Wabash River coal gasification plant operated by Connoco/Philips is similar in design to that shown in Figure 1-1 and was the planned field test site for the temperature measurement probe being developed under the DOE project. Since the Wabash River facility would serve as the field test site, this also served as the source of the coal slag used in these experiments.

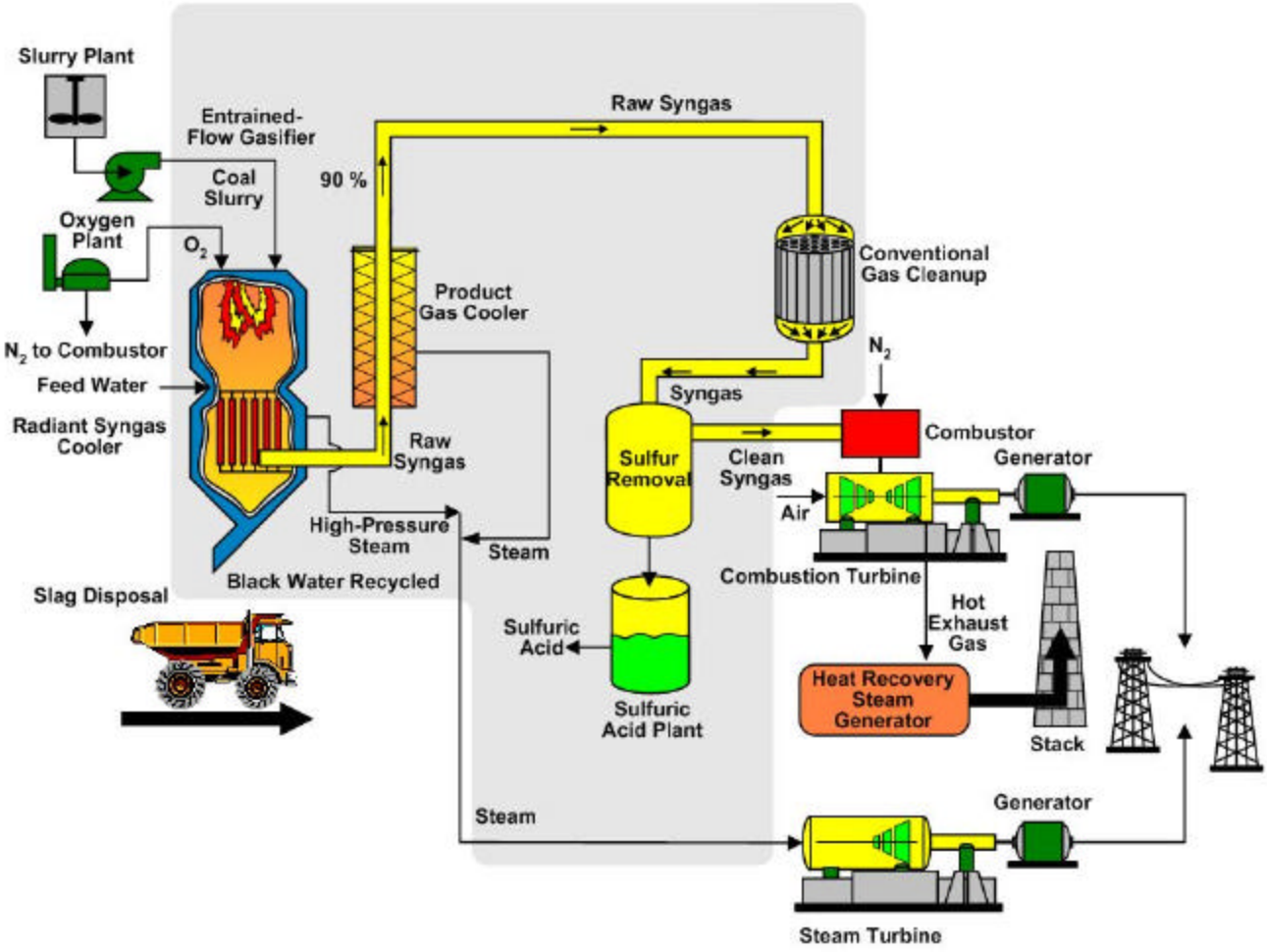

Figure 1-1- Diagram of coal gasifier and all of its products[2]

The coal gasification process has environmental and efficiency benefits over coal combustion[1]. It has the capability of removing most of the pollutants from coal-derived gases. Regarding environmental issues such as atmospheric build up of greenhouse gasses such as carbon dioxide, the gasification process also can offer an improvement. Oxygen can be used in the gasifier instead of air, (which contains about 75% nitrogen), in order to obtain a more concentrated carbon dioxide gas. In this way, it is easier and less costly to capture carbon dioxide than in the process of conventional coal burning where the gas is more diluted with nitrogen.

As far as efficiency is concerned, the fuel efficiency of coal gasification is superior to coal burning[1]. Energy generated in a coal gasification process can be used for more than one purpose. The heat from firing already cleaned gasses in a gas turbine is also used for generating steam for steam turbines in a combined gas turbine/steam turbine cycle. High efficiency in the gasification process not only produces more economical electric power, but also uses less fuel, meaning that less pollutants and greenhouse gases are produced per unit of electrical power.

Monitoring the temperature inside a coal gasifier is difficult because of the extremely harsh and corrosive environment. Coal constituents such as alkali, sulfur and transition metals together with hot steam contribute to this corrosive environment[3], in which limited temperature measurement techniques are possible. Platinum thermocouples that are currently used in the gasification process show extremely abbreviated lifetimes, sometimes lasting less than a few hours after startup. The focus of the overall program funded by the Department of Energy and in partnership with Global Energy Technology (of which the gasification business unit is now Connoco/Philips), is to develop and demonstrate a robust temperature measurement system for use in coal

gasifiers. A new broadband polarimetric differential interferometry (BDPI) based measurement technique was developed under this project for high temperature measurements. This temperature measurement system can achieve a resolution better than 0.1^{o}C based on optical birefringence based interferometric technology. The success of the temperature measurement system, however is critically tied to the performance of the materials in the coal gasification environment, and therefore requires materials that are resistant to chemical attack of the corrosive coal slag at temperatures as high as 1400^{o}C.

Figure 1-2 demonstrates the schematic design of the optical high temperature measurement system based on the BPDI technology[4]. The sensing element in this apparatus, which is made out of a material that exhibits birefringence, is placed between the polarizer and the analyzer and is oriented at a 45^{o} angle. As the light passes through it, it propagates with a differential phase delay that is due to the differences in refractive index along the *a* and *c* axes of the crystal which in this case is single crystal sapphire. The birefringence, or difference between the refractive indices in the *a* and *c* direction, and therefore the differential phase delay is a function of temperature. As a result, the signal generated by the differential phase delay contains the temperature information.

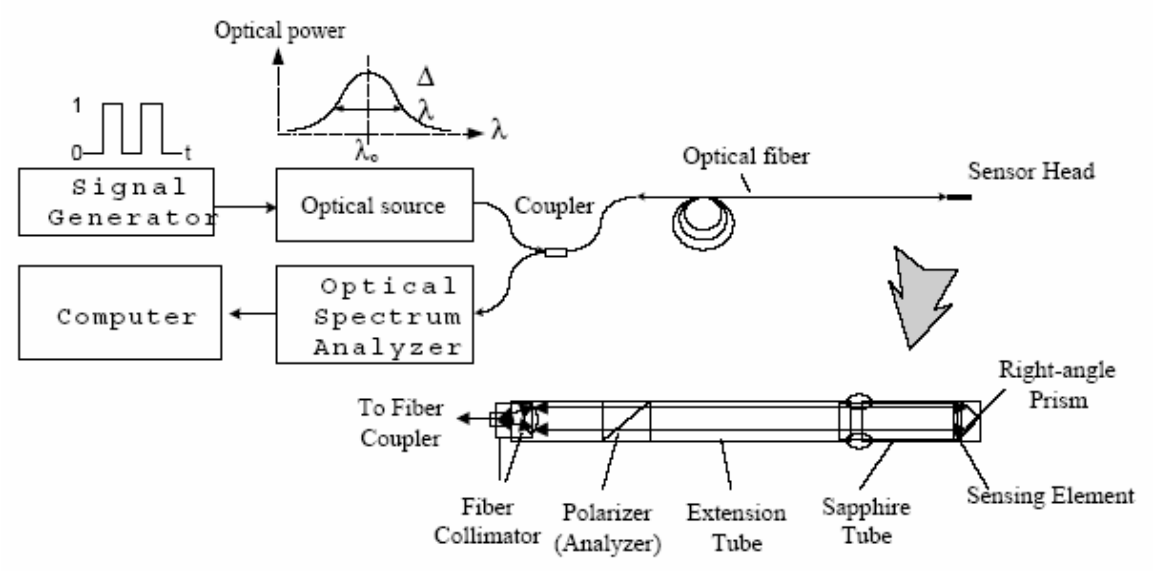

Figure 1-2- Schematic design of BPDI technology based optical high temperature measurement system[5]

Single crystal sapphire and fully stabilized cubic zirconia are candidate materials for use in coal gasifiers because of their high melting points. Because of its crystallographic structure, sapphire exhibits inherent birefringence[3] which can be utilized for temperature determination. Sapphire was chosen to be the sensing element for investigation. No data was found in the literature on single crystal sapphire corrosion in coal slags at the temperature range of interest for this work. In order to be able to better predict the performance of the sapphire in the coal gasification environment, a fundamental study of the corrosion characteristics of single crystal sapphire in coal slags was undertaken. Also, to determine if the temperature measurement technology could possibly be extended to other industrial systems such as glass melting, corrosion of sapphire and zirconia in commercial glass melt compositions was also studied.

2. LITERATURE REVIEW

2.1 Sapphire

Single crystal sapphire has unique physical, chemical and optical properties such as high melting temperature, high hardness, relatively good optical transmission windows, and optical birefringence. The combination of these properties may allow sapphire to withstand the high temperature, high pressure, thermal shock, abrasion and erosion in harsh environments, such as those found in commercial gasifiers and glass melting operations. Single crystal sapphire is chemically composed of pure aluminum oxide, Al_2O_3. Various high purity polycrystalline aluminas are also available. Sapphire has a hexagonal/rhombohedral crystal structure which determines a number of properties exhibited by sapphire[6]. The main advantage of single crystal sapphire over polycrystalline alumina is that it is non-porous and contains no grain boundaries. Therefore use of single crystal sapphire will eliminate the effect of corrosion along the grain boundaries. The melting point of sapphire is 2053°C[7] and it is able to withstand extreme thermal shock conditions due to its high strength and high thermal conductivity[8]. Sapphire is an attractive optical material. Its large energy gap of 9.1eV enables it to have superior optical transmission compared to other oxide materials. In addition, sapphire has the ability to transmit at extremely high temperature. Sapphire has exceptionally high chemical stability even at high temperatures in oxidizing environments. It is the hardest oxide material. It's hardness of 9 on Mohrs scale, closely compares to that of diamond, which is 10.

In summary, sapphire is one of the strongest and hardest oxide materials available, with exceptional chemical resistance, good thermal shock properties

and high temperatures stability, and desirable optical characteristics. For these reasons, it is a material of choice for optical applications in harsh environments.

2.1.1 Corrosion of sapphire

There are many publications on corrosion of polycrystalline alumina in different surroundings. One of the conclusions in most of those investigations was that the corrosion of the polycrystalline alumina samples occurred preferentially along the grain boundaries. T. Oh, L. N. Shen, R. W. Ure, Jr. and I. B. Culter investigated the corrosion of dense alumina and high purity magnesium aluminate spinal in coal slag[9]. They used two compositions of coal slag: first slag consisted of Al_2O_3, SiO_2 and CaO, while the second slag contained Fe_2O_3, K_2O and MgO in addition to Al_2O_3, SiO_2 and CaO. They observed the penetration of slag into alumina along the grain boundaries. The rate controlling step in the corrosion process was mass transport of refractory material away from the interface through the slag.

Since this seems to be one of the most prominent attacks to alumina, it would be of great importance to investigate the corrosion mechanisms of single crystal alumina, where there is no effect of grain boundaries, and to determine the extent of corrosion and which corrosion mechanisms take place. Tea-Il Oh[10] states in his master's thesis that the existence of grain boundaries does not significantly affect corrosion rates. Nonetheless, the penetration of the impurities does take place along grain boundaries. A 100μm layer was identified in the sample of alumina, which was treated in the first coal slag at 1420^{o}C for 7 hours. Another sample measured 900μm erosion after 50 hours in the first slag for 1450^{o}C. These experiments on dense polycrystalline and single crystal alumina in the same slag indicate only a small variation. Since

the corrosion was controlled by diffusion of material through the boundary layer, more rapid attack of the slag through the grain boundaries does not play a significant role. He adds that slag penetration into oxide refractories will strongly alter mechanical properties. Creep and spalling will increase due to the different thermal expansions of the slag that penetrated through oxide refractory.

2.1.2 Sapphire in silica melts

A. R. Cooper and W. D. Kingery[11] investigated factors that determine rate of dissolution of sapphire in CaO-Al_2O_3-SiO_2 slag at temperatures between 1340^{o}C and 1550^{o}C during forced and free convection. Their experiments showed that the mass transport in silicate melts away from the interface controls dissolution of sapphire based on density difference as a driving force. This conclusion was also consistent with tracer diffusion data for the silicon ion and is true even for the forced convention experiments where the rotation of the specimen causes mass transport to take place at a higher speed. In the case of stationary specimens, after a short period the dissolution of sample in the glass melt becomes independent of time and takes place at steady state rate, meaning that the rate of diffusion does not change with time. It was noted that in free convection there is a significant increase in degradation of the sapphire sample at the slag-ambient interface. This phenomenon is believed to be caused by surface forces that increase with increasing Al_2O_3 content. As sapphire slowly dissolves in the slag, the Al_2O_3 concentration increases around the sample which causes the increase in surface forces which are responsible for enhanced corrosion.

In the continuation of the previous work, B. N. Samaddar, W. D. Kingery and A. R. Cooper examined dissolution of sapphire, dense alumina, mullite,

fused silica and anorthite in $CaO-Al_2O_3-SiO_2$ slag at 1350°C and 1500°C at free and forced convection[12]. They found that the dissolution rates are controlled by the diffusion through the boundary layer. At 1350°C sapphire and polycrystalline alumina degrade at the same rate, but much slower rate than the other materials studied. This observation indicates that the presence of grain boundaries did not have an effect on the corrosion rates under the conditions studied. At 1500°C, the sapphire and polycrystalline alumina both showed similar data values that follow the same best fit line. In addition, they demonstrate far better corrosion resistance than mullite and vitreous silica. It was observed that for the forced convection at the initial time of the reaction, the corrosion rate of polycrystalline alumina was higher than that of sapphire, but after 20 minutes the corrosion rate was the same. The conclusions of the authors of this work indicate that the rate controlling step of sapphire corrosion in molten calcium-aluminum-silicate slag is the dissolution of sapphire through the boundary layer. The thickness of this boundary layer is dependant on the hydrodynamics. This conclusion was based on the observation that rates of dissolution were greater under forced convection than in the case of free convection. No new solid phases were observed at the interface. The boundary layer in the liquid phase might indicate a formation of a metastable phase.

K. H. Sandhage and G.J. Yurek examined dissolution of sapphire in $CaO-MgO-Al_2O_3-SiO_2$ slag at 1450°C and 1500°C, and the growth of magnesium-aluminate spinel as the interface product. They prepared 5 different slags with varying composition of components. Although all of those components are known to have a severe corrosive effect on the refractories, the slag that contained the greatest CaO content exhibited the greatest degradation of the sapphire. The 3 slags that contained the most MgO formed a magnesium aluminate spinel layer. In addition, this interface layer was observed to

increase in thickness with increasing temperatures for a constant reactions time. The authors state that there is two parallel processes taking place in the corrosion of the sapphire in the calcia-magnesia-alumina slags: formation of an aluminate spinel layer at the interface and its dissolution in the slag. The process that controls this reaction is diffusion of the spinel product into the slag. Just like in the previous papers described, this work confirms that this process is driven by the density difference. The interesting observation in this paper is that there was less degradation of sapphire in the lower parts of the sample. This is the result of the dissolution of sapphire, which is essentially alumina, into the slag and its flow through the slag. As the sapphire was dissolving, the concentration of alumina in the slag immediately next to sapphire sample increases. Therefore, alumina was flowing downward, becoming denser in the lower parts and essentially protecting the sample from the calcia and the magnesia slag constituents.

2.1.3 Sapphire in Coal Slag

M. K. Ferber and V. J. Tennery[13] examined behavior of structural ceramics in hot combustion gases from coal-oil mixtures at 1240^{o}C for 240 hours. The slag they worked with consisted primarily of Ca, Si, Al, Fe, and Mg, but it also included small quantities of Ti, Na and K. They noted the reaction product of about 25μm uniformly distributed at the alumina surface. This boundary layer mainly consisted of alumina and iron, but traces of nickel were also observed. This led to the conclusion that iron-nickel aluminate spinel was forming at the alumina interface. Further dissolution of this interface product in the slag was also noted as a stage during the corrosion process. The micrographs indicate the existence of block like crystals inside the coal slag. Those block crystals were found to consist of iron and were only present after

the heat treatment of alumina. It is suspected that they originate from dissolution of the iron-nickel aluminate interface product.

2.2 Zirconia

Pure zirconia (ZrO_2) does not occur in nature. It is found in baddeleyite and zircon ($ZrSiO_4$). Out of these two sources, zircon is more abundant, but less pure and therefore requires a significant amount of processing to yield zirconia[14]. At room temperature, pure zirconia exists in the monoclinic form. To make zirconia stable at elevated temperatures, it has to be transformed to the cubic or the tetragonal phases. Phase transformation from the monoclinic phase to the tetragonal phase occurs at 1170°C and to the cubic phase at 2400°C[15]. Due to the large change in lattice size during this phase transformation and thus a volume expansion, it is difficult to use zirconia at high temperatures. In order to manufacture zirconia and avoid the detrimental phase transformations, it has to undergo extensive modifications, mainly to be transformed to the cubic form. This can be accomplished by addition of stabilizers such as calcia, magnesia, and yttria. Zirconia can become stable at lower temperature by doping it with a stabilizing agent. When zirconia has been transformed from a monoclinic to the tetragonal phase as a consequence of doping, it is referred to as partially stabilized zirconia or PZT. Further doping will result in transformation into cubic phase, called fully stabilized zirconia. Figure 2-1 represents the phase diagram of the yttria-zirconia system[16].

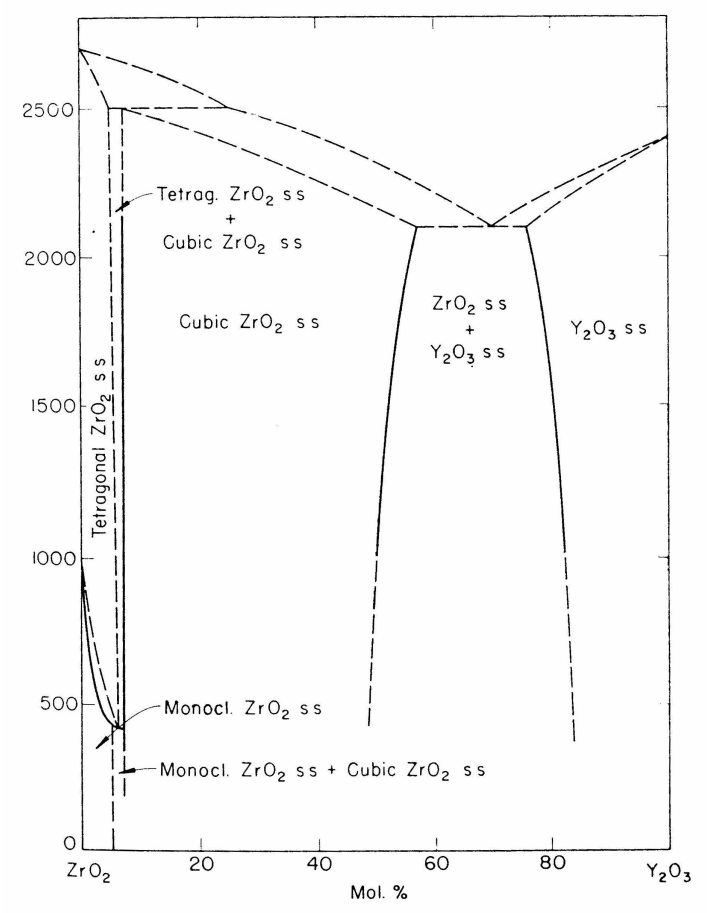

Figure 2-1- Phase diagram of yttria-zirconia system[16]

Partially and fully stabilized zirconia can be processed to exhibit exceptional properties such as high strength, hardness, and fracture toughness, excellent wear and chemical resistance, and has been used for a number of applications in many areas. These properties can be further modified by the amount and type of stabilizer.

Many types of zirconia have been developed by exploiting properties of various phases. Some examples of different types of zirconia are: Tetragonal Zirconia Polycrystals (TZP), Partially Stabilized Zirconia (PSZ), Fully Stabilized Zirconia (FSZ), Transformation Toughened Ceramics (TTC), Zirconia Toughened

Alumina (ZTA), and Transformation Toughened Zirconia (TTZ)[17]. Some phases are stable only at high temperatures without addition of stabilizing agents. The stability of different polymorphs of zirconia has been examined by many authors[15,18,19,20,21].

Another direction of improving zirconia materials is through toughening mechanisms. The volume expansion which occurs as a result of the phase transformation can be used to produce zirconia with enhanced toughness. This material, also known as transformation toughened zirconia or TTZ, is in the form of a composite where the cubic zirconia matrix is reinforced with tetragonal zirconia particles[3]. This structure utilizes the volume expansion as the tetragonal particles transform to monoclinic at the deformation zone which toughness the material. Much work has been done in this area for various materials systems. For example Nishida A. and Terai K.[22] used this property to improve the strength of MgO-ZrO_2 composites. The microcracks that were formed during the cooling process after sintering were closed up as a result of the volume expansion of the zirconia as it transformed from tetragonal to the monoclinic phase, the stable phase at lower temperatures.

All types of zirconia are well tolerable of thermal gradients. The comparison of thermal expansion coefficient and thermal conductivity of zirconia and other materials is presented in Figure 2-2.

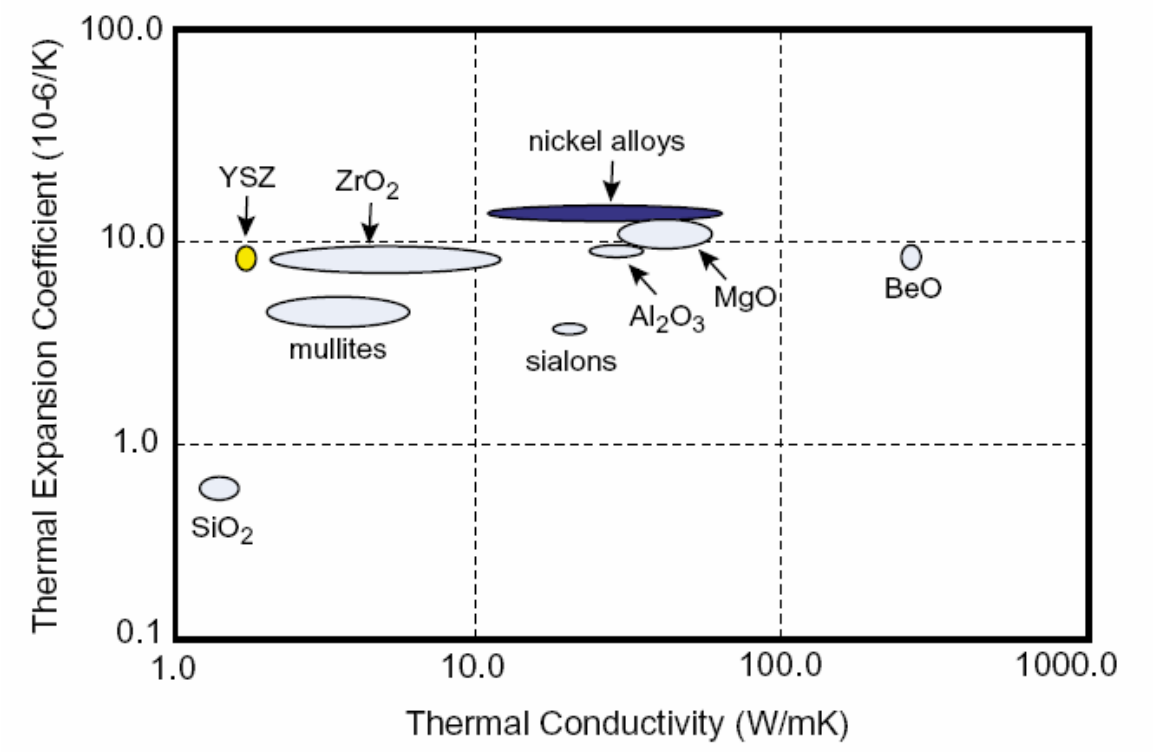

Figure 2-2- Plot of thermal conductivity vs. thermal expansion coefficient. YSZ has a CTE = 9.0 x 10-6 K-1.[23]

In addition zirconia has better performance than most conventional components in corrosive, abrasive and erosive environments[24]. Due to its low degradation in acids and alkali, and high strength and hardness, zirconia may make a good candidate material to utilize in high temperature corrosive environments.

2.2.1 Corrosion of zirconia in different slags

V. K. Pavlovskii and Yu. S. Sobolev et al[25] investigated corrosion of single crystals of alumina, silica and tetragonal zirconia stabilized with yttria, in high lead glasses. They prepared two different compositions of glasses: one with a mass fraction of 66% of lead and the other with 85%. The corrosion of sapphire, silica and zirconia specimens was conducted at 1300^{o}C for 24-72

hours in lower lead content glass and at 1000°C for 6-12 hours in higher lead content glass. Zirconia exhibited the highest corrosion resistance in these experiments. The corrosion rate of zirconia in 85% lead glass was approximately three times higher than in 66% lead glass. The surface analysis showed an interesting micro-structural formation: a layer of zirconia of a size up to 100μm, separated from the specimen. This layer, also known as baddeleyite, has higher zirconia content than in the specimen and much lower yttria content. The specimens corroded for longer time periods demonstrated thicker separation layer and lower yttria content. The reason for this behavior is that lead diffuses into the zirconia sample, destabilizing it and replacing yttria. The yttria content decreases and zirconia becomes more concentrated than in the original sample. The zirconia structural changes from tetragonal to monoclinic and it is accompanied by a volume expansion which explains the thickening of the separated layer. This phase transformation also causes cracking at the surface. In the case of the high lead content glass, an alternate structure of baddeleyite and glass was formed.

M. Yoshimura, T. Hiuga and S. Somiya[21] studied reactions and dissolution of single crystal yttria stabilized zirconia in acidic and basic solutions at 600°C and 100MPa. Most basic solutions had little effect on zirconia. In KOH, NaOH and LiOH partial decomposition of zirconia was observed. However, under acidic conditions (Li_2SO_4, H_2SO_4 and HCl) yittria stabilized zirconia was completely decomposed into monoclinic zirconia. The reason for this transformation is that yttrium ions are more basic than zirconium ions and therefore they dissolve in the acidic environment faster. After the yttrium ions are depleted, zirconia transforms into its polycrystalline monoclinic phase.

Y. D. Chang and M. E. Schlesinger[26] examined corrosion of polycrystalline calcia and magnesia partially stabilized zirconia in CaO-FeO-SiO_2 slags. Three

different slag compositions were used. Slags that were less basic and had high FeO content extracted magnesia from the zirconia matrix which finally resulted in dissolution of zirconia samples. In the case of calcia stabilized zirconia, immersion of the samples into the slag even for short time periods resulted in complete destruction of the sample. Both static and rotating experiments were conducted for all slag compositions and interestingly, the corrosion rate of rotating samples was found to be equal or less than for static samples. The most basic slag out of the three resulted in the greatest corrosion. However, this slag resulted in no destabilization of the cubic phase. It was further concluded that degradation of zirconia occurs without prior phase change. This conclusion can be supported by the fact that enhanced corrosion rates under dynamic conditions in highly basic slags confirm that the rate controlling process in corrosion is the diffusion of zirconia through the boundary layer.

Many studies have been done on corrosion effects of different elements or environments on single crystal sapphire and zirconia. A variety of slag compositions were used in those studies to examine sapphire and zirconia corrosion. There have been studies on corrosion effects of coal slag on various oxide refractories as well. Nevertheless, so far, there has been little or no data in the literature on corrosion of single crystal sapphire and zirconia in coal slag and soda lime glass at elevated temperatures. Due to the lack of available date, the present study was undertaken.

3. EXPERIMENTAL PROCEDURE

The focus of the experiments in this research project was to measure the amount of corrosion of single crystal sapphire and zirconia in corrosive slags at high temperature and at various time periods. The thickness of the samples was measured before and after corrosion experiments. Their difference represents the amount of corrosion.

3.1 Materials Selection

Materials and equipment used to conduct corrosion experiments of sapphire and zirconia in coal slag and glasses are shown in this section.

Table 3-1- Table of materials

MATERIALS	***SOURCE***	***QUALITY***
Sapphire	Saphikon	n/a
Zirconia	Ceres	Fully stabilized cubic, 20wt% Y
Sand	Aldrich	50-70 mash
Aluminum oxide powder	Aldrich	99.70%
Calcium oxide	Aldrich	n/a
Boric acid	Aldrich	99+%
Sand, white quarts	Aldrich	50-70 mash
Zirconium oxide	Aldrich	n/a
Strontium oxide	Aldrich	99.9%
Sodium tetraborate	Aldrich	99%
Sodium carbonate	Aldrich	99.5+%
Coal slag	Wabash River	discussed in next section
Hydrofluoric acid	J.T.Baker	47, 0-52.0%
Alumina cement	n/a	n/a
Silica rods	n/a	n/a
Alumina crucibles (50mL)	Coors Tek	n/a
Alumina crucibles (5mL)	Coors Tek	n/a

Table 3-2- Table of equipment

EQUIPMENT	***SOURCE***	***PARAMETERS***
Linear Precision Diamond Saw	Buehler Isomet 4000	3500rpm, 1.2mm/min
SEM and EDX	Chem department	20kV
High temperature furnace	Deltech	1200-1400^{o}C
Vernier Caliper	Mitutoyo	0.01mm
Alumina polishing paper	Ultra Tec	30u

3.2 Coal Slag

The coal slag which is from the Wabash River coal gasification facility consists of many corrosive components. In this investigation, it was important to identify those components in order to attempt to identify the corrosion mechanisms which take place. A spot scan performed on the coal slag using SEM/EXAX is shown in Figure 3-1. This figure indicates that the coal slag used for the corrosion experiments consisted mainly of Silicon, Aluminum, Iron, Potassium and Calcium in that order of abundance.

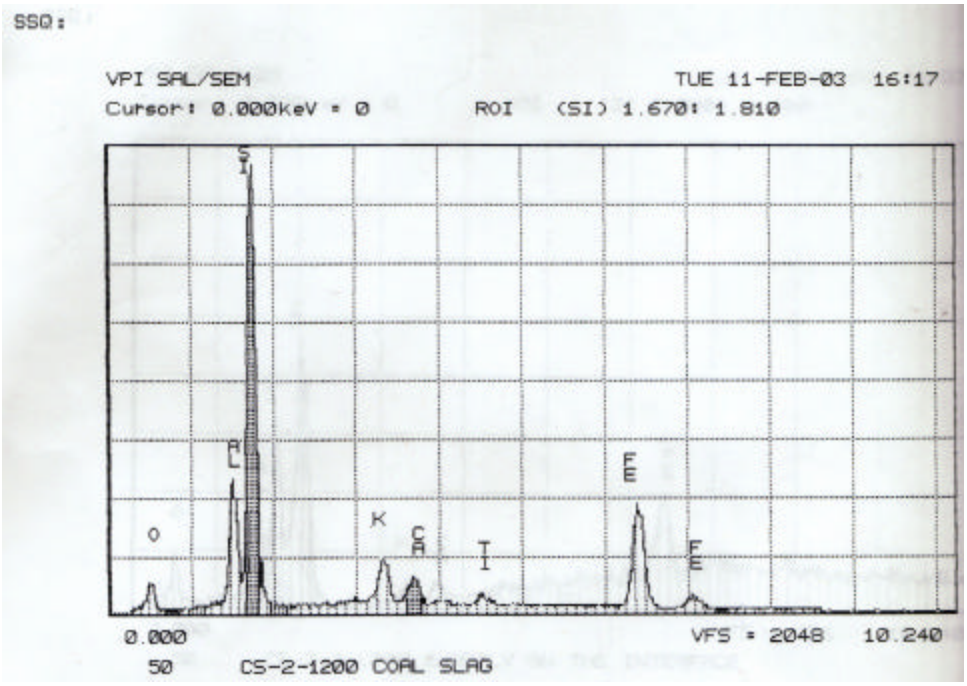

Figure 3-1- composition of coal slag

3.3 Soda Lime Glass

Soda lime glass was obtained by crushing a commercially available glass bowl. The spot scan obtained reveals the relative abundances of the elements present, Figure 3-2. Soda lime glass that we used for the experiments is rich in silicon, and contains smaller amounts of sodium, calcium and aluminum.

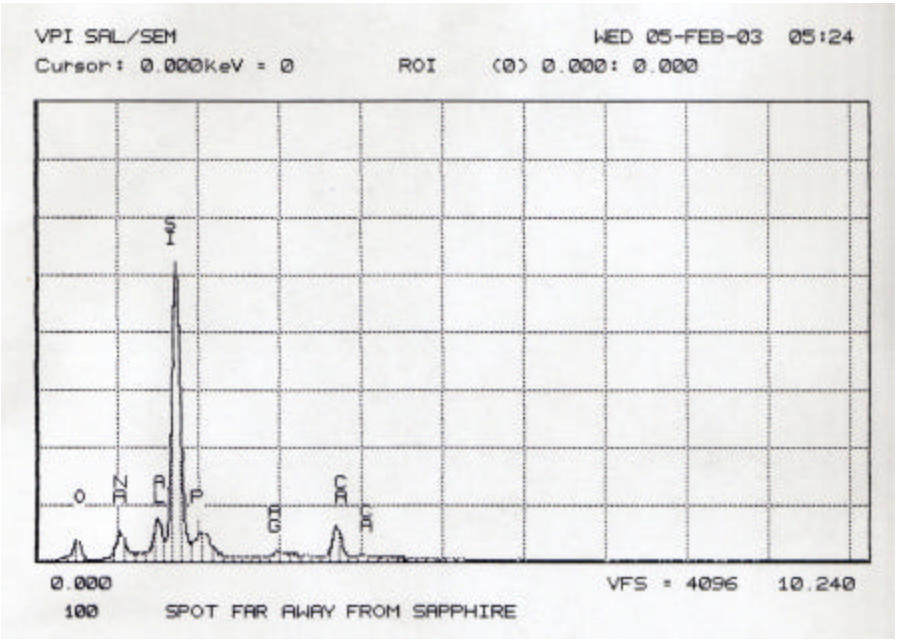

Figure 3-2- composition of soda lime glass

3.4 Sample Preparation

All corrosion experiments for the sapphire and zirconia in different environments were obtained in similar fashion as described in this section.

Single crystal sapphire plates (about 0.8mm thick) were cut using a diamond saw (Figure 3-3) into samples approximately 5cm x 1cm x 0.8 mm. Zirconia samples were cut from a bigger zirconia crystal also with the diamond saw. Zirconia samples were uneven in thickness due to difficulties in clamping

and cutting of the zirconia crystal in the saw. These samples were approximately 3cm x 0.8cm x 1mm.

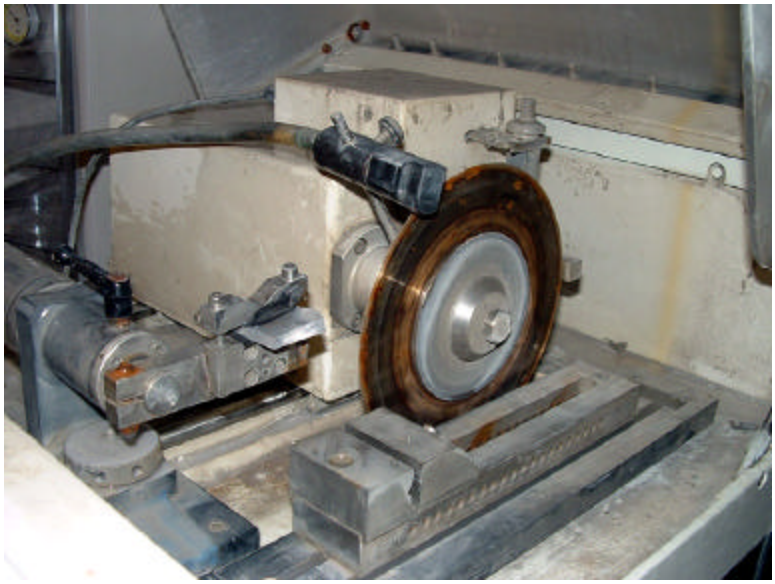

Figure 3-3- Diamond saw

Soda lime was obtained by crushing a soda lime glass bowl into small pieces. Borosilicate glass was made from powders. The coal slag did not need any special preparation; it was already small in size and suitable for the experiments.

3.5 Heat Treatment

One sapphire sample and one zirconia sample were placed in a 5mL alumina crucible, Figure 3-4 (a). The crucible was then filled with the corroding material: coal slag, Figure 3-4 (b), crushed soda lime glass, Figure 3-4 (c) or mixed borosilicate glass. The heat treatment was conducted in a Deltech Inc.-furnace, shown in Figure 3-5, at 1200^{o}C, 1300^{o}C and 1400^{o}C for four

different time periods: 1 day, 2 days, 3 days and 4 days. For all temperature and time conditions, the temperature was ramped at the rate of 5^{o}C per minute, held at the specified temperature for the specified time and then ramped down to room temperature at the rate of 5^{o}C per minute. Slow heating and cooling rates were important for the life of heating elements in the furnace as well as for preventing cracking of the sapphire and zirconia samples due to thermal expansion mismatch with the solid glass or coal slag.

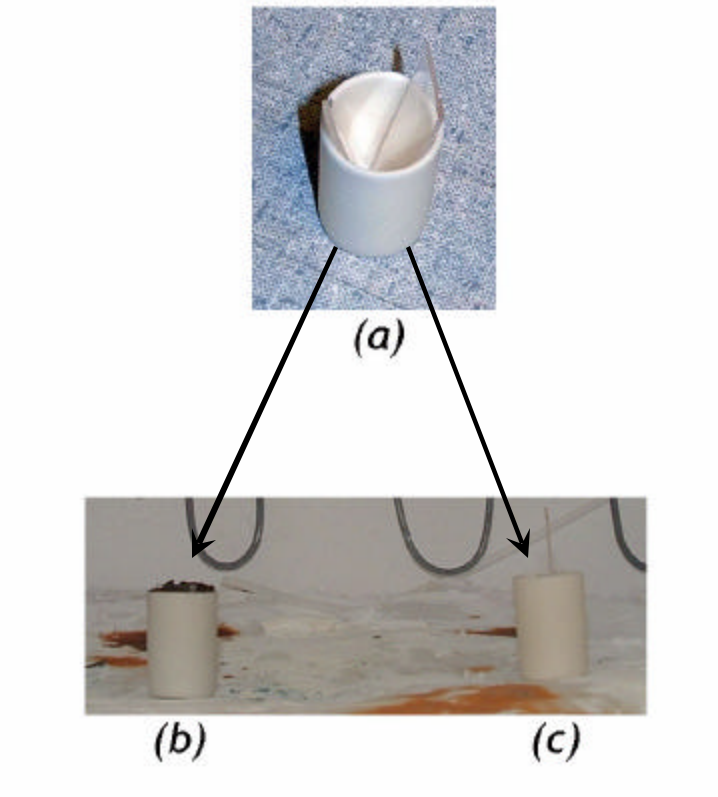

Figure 3-4- Samples of sapphire and zirconia in: (a) empty alumina crucible, (b) coal slag and (c) soda lime glass

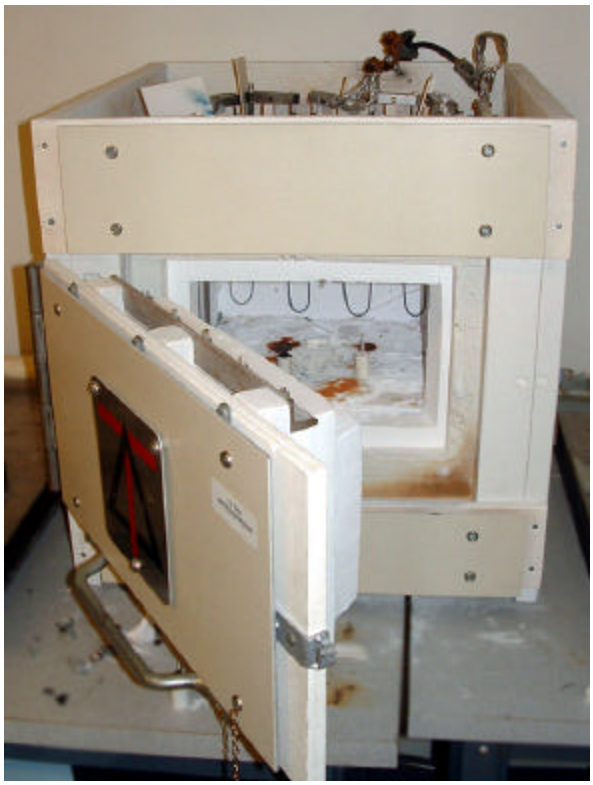

Figure 3-5- Furnace

After the heat treatment for a couple of days at high temperature, samples of sapphire and zirconia were often cracked and yellowish in color, most likely due to the presence of iron in the slags. The coal slag had trapped gas bubbles during solidification and only about half of its volume remained inside the crucible after heating. Figure 3-6 shows the sample of sapphire after the heat treatment.

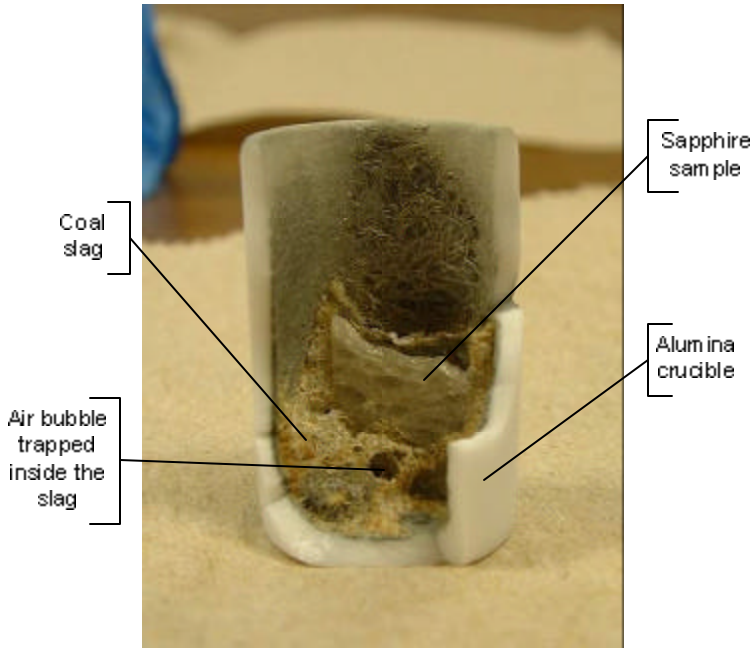

Figure 3-6- Sample of sapphire in coal slag after the heat treatment

3.6 Thickness Measurements

Upon cooling, using a diamond saw, the slices were cut from the crucibles that included the sample (sapphire or zirconia) –slag (glass or coal) interface, Figure 3-7 and Figure 3-8.

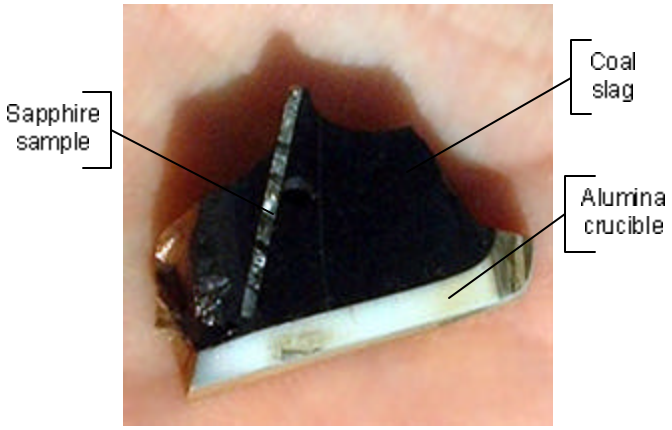

Figure 3-7- Cross sectional cut of sapphire in coal slag

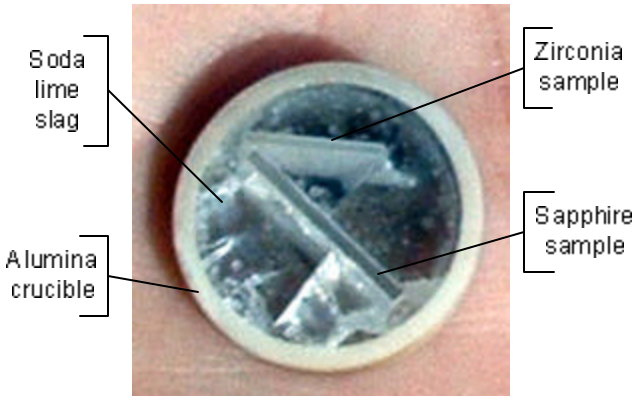

Figure 3-8- Cross sectional cut of sapphire and zirconia in soda lime glass

The initial thicknesses were measured simply with a Vernier caliper. The final thickness, however, was more difficult to measure. Two methods were employed to measure the final thickness- dissolution of the slag with hydrofluoric acid method and SEM method.

3.6.1 HF Method

One circular cross section of the crucible including the slag and the sample of the sapphire and the zirconia was placed in concentrated hydrofluoric acid until all slag was dissolved. The sapphire and zirconia pieces were then polished with alumina polishing paper to make sure that all of the slag was removed from their surface. The samples were washed with DI water. After the samples dried, the final thickness measurements were conducted with a Vernier caliper. Then measurements were taken for each sample and the average value and standard deviation recorded. This method worked better for coal slag than for soda lime glass because coal slag was easier to dissolve. It took roughly two weeks to dissolve the coal slag and four weeks to dissolve the soda lime glass, depending on the quantity of the material that was to be dissolved. Some samples in soda lime took more than 6 weeks. It is suspected that this is because the soda lime could have reacted with HF

forming a white residue and neutralizing the HF acid. This residue is soft and the outside of it could be removed by scraping. Then the sample was returned to the HF and when the outer part becomes soft, it was scraped off, and so on.

To assure that the accuracy of the final thickness measurements, the repeatability measurements of sapphire and zirconia alone in concentrated hydrofluoric acid were obtained. A sample of uncorroded single crystal sapphire and zirconia were placed inside a plastic container which was then filled with concentrated hydrofluoric acid. The samples were left in hydrofluoric acid for ten days. The thicknesses of the sapphire and zirconia samples were measured with a Vernier caliper before and after the HF acid treatment. The average thickness obtained did not change after ten days in hydrofluoric acid. This repeatability measurement shows that the thickness of the sapphire and zirconia samples were not affected by the hydrofluoric acid, indicating that hydrofluoric acid does not dissolve sapphire and zirconia and it is safe to leave the samples in it in order to dissolve the slag. This was an important measurement because it insures that concentrated hydrofluoric acid did not influence the repeatability of thickness measurements of sapphire and zirconia samples in any way.

In addition, to determine the repeatability of the measurement process, repeated measurements were conducted on a sapphire sample. A series of 10 measurements was performed on the same spot of the sample. All 10 data points were identical and standard deviation of zero was obtained. The sample process was repeated on another 2 samples, and again, all the measurements had the same value. However, the samples were broken after the heat treatment, and a series of measurements was performed on each piece that was big enough to measure. The average value of all the pieces represents the final thickness. Since not all of the measurements were the same in this case,

the standard deviation was calculated for each sample. The standard deviation bars are shown in Figure 4-1.

3.6.2 SEM Method

Scanning Electron Microscopy (SEM) was used to take pictures of the sapphire and zirconia samples in the slags. Circular cross sections of the crucible (including the slag and the sample) were placed inside the SEM chamber in the way so that the scanning angle would be perpendicular to the sample. This initial set up is important because if the angle deviates from 90^{o}, the picture taken would be distorted and the measurements taken from it would be inaccurate. Pictures were taken of a section that includes both left and right interfaces of sample. Since this is a cross-section of the crucible containing the sample, the part of the sample viewed is the thickness. Then the thickness of the sample shown on the picture was measured with a ruler and multiplied by the scanning magnification to obtain the final thickness of the sapphire specimen.

3.7 Complexity of high temperature corrosion experiments

Lastly, the difficulty of the heat treatments and thickness measurements should be emphasized. High temperature corrosion experiments are complex and not easy to conduct. The heat treatments require a reliable high temperature furnace with accurate temperature reading system inside. The dwelling temperatures constant as set and the ramping speed should be steady. Any sudden jumps in temperature can easily cause cracking in the samples.

Thickness measurements represent the amount of corrosion, and they involved etching in concentrated hydrofluoric acid. On many occasions, the

cracking was so intense that after the slag was dissolved in the hydrofluoric acid, the samples zirconia would turn into small pieces, which could not undergo any reasonable measurements. Sapphire samples also experienced certain amount of cracking, although it did not affect the measurements. Numerous samples had to be prepared and heat treated in order to get a single sample that was measurable. Removing soda lime glass from the samples was especially difficult. The product formed between this glass and HF acid had to be removed with sand paper which caused even more cracking. It was hard to decide if this residue was completely scraped off or not. It was essential to use sand paper as few times as possible because any additional scraping could have resulted in loosing the sample.

In this study, all of the data that had been obtained was collected and used to obtain the amount of corrosion of sapphire and zirconia in corrosive slags at high temperatures.

Some samples showed more variation in the data than others. Possible reasons for variation are discussed in Section 4.4.

4. RESULTS AND DISCUSSION

4.1 Sapphire

After reacting sapphire in corrosive slags for various time periods (1 to 4 days) at high temperatures (1200^{o}C, 1300^{o}C, and 1400^{o}C), thickness measurements were obtained. The difference between the thickness after the corrosion and the thickness before the corrosion indicated the amount of degradation of sapphire in the slag. Overall, sapphire showed very little degradation in both coal slag and soda lime glass at high temperatures. Cracking and surface defects were observed in samples treated at higher temperatures such as 1400^{o}C.

4.1.1. Sapphire in Coal Slag

Conducting corrosion experiments of single crystal sapphire in coal slag was meant to simulate the exposure of sapphire sensors in corrosive coal gasification environment. Obviously, many differences exist between the laboratory testing and operation in the real gasification environment, but the data obtained from those experiments can be extrapolated to show the estimated behavior of the single crystal sapphire in the coal gasifier at different temperatures and at longer time periods.

4.1.1.1 Thickness Data

Table 4-1 summarizes the data obtained from the HF acid etch method and the SEM method. Since the data is not consistent for these two methods, the HF method was chosen as the more reliable one and the rest of the

measurements were conducted using only this method. There are two reasons for choosing the HF etching method to be more dependable. The major reason is that the SEM method gave distorted measurements. The thickness observed with the SEM depended on the angle at which the sample was tilted inside the crucible, and the angle of the cut. Since this angle was difficult to measure, the true thicknesses of the specimen after corrosion were not obtained with this method. The detailed explanation of the SEM method deficiencies is discussed in the error analysis, Section 4.4. The second reason for choosing the HF method was that the HF method was able to provide multiple measurements on one sample which could then be averaged. The SEM method could only give measurements along a single cross section of the sample.

The data from the HF method indicated that there was very little corrosion taking place. This data does not exclude the possibility of formation of an interfacial product which, if it exists, diffuses away from the interface over time. For example, the sapphire sample that was immersed in coal slag for 1 and 2 days at 1300^{0}C might have formed an interfacial product which did not have a chance to diffuse away yet before the experiment was stopped and the slag solidified. After four days in coal slag the sapphire shows more degradation which could be due to the interfacial product dissolving in the coal slag. Considering the very small values of the thickness changes before and after the corrosion, it is uncertain whether there is an existence of any interfacial reaction products or not. Most likely the variation in thickness from zero is due to experimental errors.

Table 4-1- Change in thickness of sapphire in coal slag

	HF method			***SEM method***		
Days in furnace	***1200^{o}C***	***1300^{o}C***	***1400^{o}C***	***1200^{o}C***	***1300^{o}C***	***1400^{o}C***
1	-0.01	0.01	0.02	-0.0827	0.0615	
2	-0.01	-0.01	0.05	0.0387	0.0427	
3	0	-0.02	0.04	0.0476	0.0385	
4	0.01	-0.01		-0.0505	-0.0497	-0.1025

Figure 4-1 represents change in thickness of single crystal sapphire versus reaction time and temperature in coal slag. The data points show the minimal variation from zero. The flat plot curves indicate no corrosion taking place. The standard deviation was also obtained among all the measurements that were taken. Figure 4-1 also shows that the amount of variation among the different data points is in the range of variation within one data point. The variation within the data point is presented as standard deviation bars in this plot. This is an indication that the variation was influenced by experimental and measurement errors and not by corrosion.

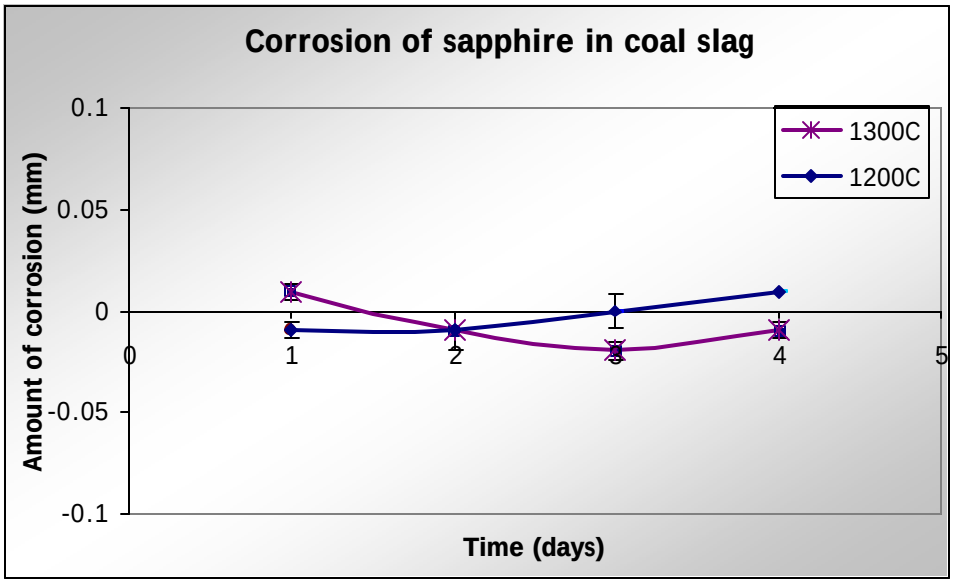

Figure 4-1- Change in thickness versus reaction time and temperature for single crystal sapphire in coal slag

4.1.1.2 Surface and interface analysis

Since the thickness data shows very little or no corrosion of single crystal sapphire in the coal slag, the SEM micrographs were used to examine the interface features such as existence of reaction products, spalling and cracking.

The least severe condition for corrosion experiments was at 1200^{o}C over a one day period. The SEM micrograph of a sapphire sample that underwent such a treatment is presented in Figure 4-2. The yellow highlights emphasize the interfaces between the sapphire sample and the coal slag. Even though the thickness measurements show no corrosion of sapphire at these conditions, there is an interesting feature on this micrograph indicating a large crack partially along the interface and partially inside the slag. The crack along the interface indicates spalling due to the difference in thermal expansion

coefficient between the sapphire and the slag. It is unusual that a thin layer of the slag remained on the sapphire while the rest of the slag separated. A small part of the slag on the sapphire was observed on the other side of the interface as well (bottom interface), where the rest of the slag completely separated. This could be related to the iron segregation that has been observed at the sapphire slag interface as will be discussed later.

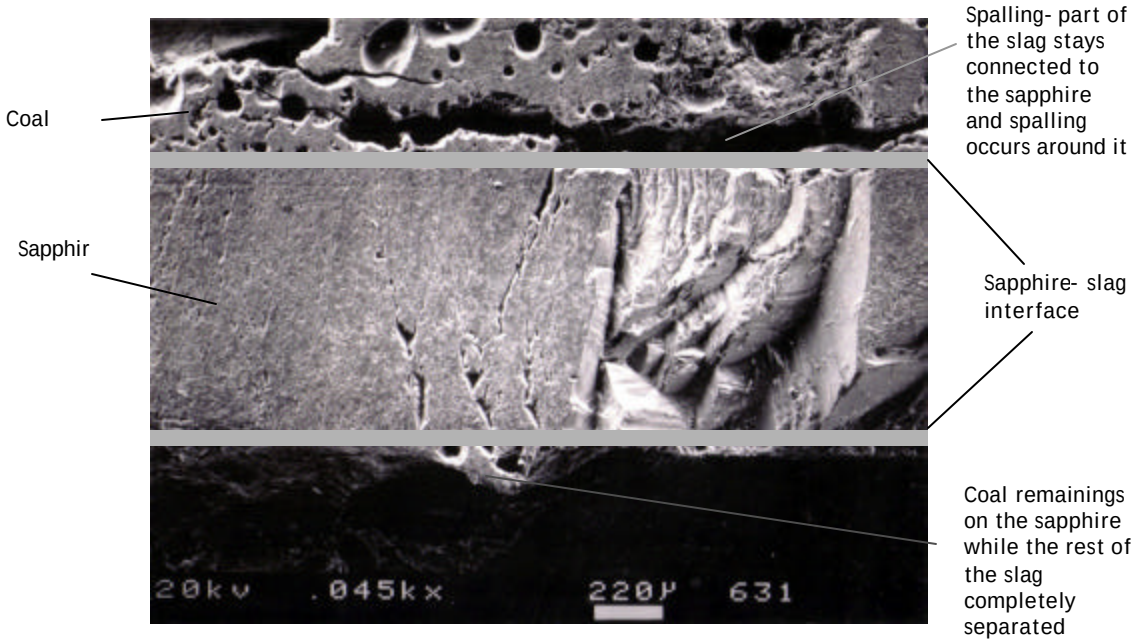

Figure 4-2- SEM micrograph of sapphire corrode in coal slag at 1200°C for 1 day

The elemental analysis of the interface was performed as well. When scanning the sapphire in coal slag, aluminum, silicon and iron are the most important elements to look for because sapphire is essentially aluminum oxide, and silicon and iron are the most abundant constituents of the coal slag used in these experiments (Figure 3-1). The forth element was chosen to be one other element found in coal slag: Ca or O. Neither oxygen nor calcium shows any important remarks. The interesting observation of many EDX scans of samples in coal slag was that iron and silicon were separated from each other. It is

obvious in those scans that spots where silicon is missing are filled with iron and vise versa (Figure 4-3, Figure 4-4, and Figure 4-8). Some scans show uniform layer of iron deposition on the sapphire surface, which may indicate the formation of iron aluminate spinel at the interface (Figure 4-3 and Figure 4-4). Nevertheless, the sapphire interface appears strait and clear, and there is no observation of iron penetrating into the sapphire sample. The aluminum scan also reveals an obvious line between the sapphire and the slag. The relative amount of the aluminum in the sapphire is greater than in the coal slag, and naturally, this shows up in the scan. The calcium scan is not a good representative of this study. This scan can falsely be interpreted as a proof of calcium penetration into the sapphire. However, this is not the case. The amount of calcium in coal slag is very small, almost neglectable, and sapphire contains no calcium. This EDX scan displays relative amounts of calcium in sapphire and coal slag. Because of the very low calcium concentration in the slag, some dots show up on the sapphire side due to the detectability limit of the scan.

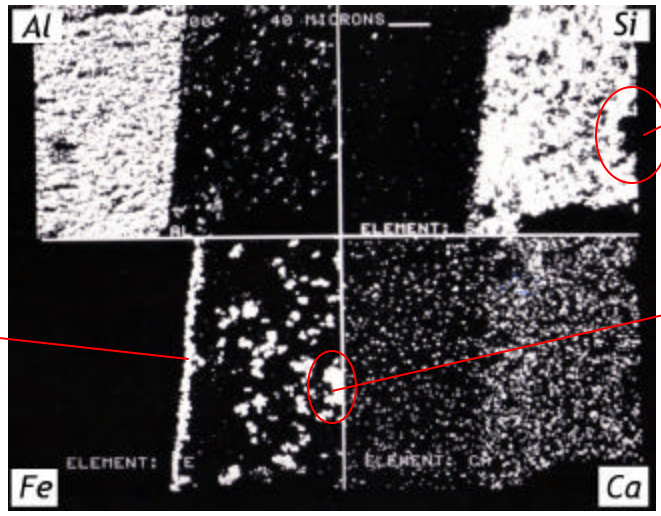

Figure 4-3- EDX scan of sapphire- coal slag interface after corrosion at 1200°C for 1 day (LEFT: sapphire, RIGHT: coal slag)

Figure 4-4 illustrates similar features as Figure 4-3. Again a uniform layer of iron right at the sapphire surface occurs and this region is depleted of silicon as shown in the silicon scan. In both the silicon and iron scan, there are traces of those elements on the sapphire side. This is most likely due to depositing of the interfacial constituents from the diamond saw onto a crack in the sapphire sample that occurred during slicing of the samples with diamond saw. The oxygen scan in this figure does not reveal any important information. It only shows that there are oxides on both sides, which can be aluminum oxide on sapphire side, and oxides or iron, silicon and other constituents of coal on the coal side.

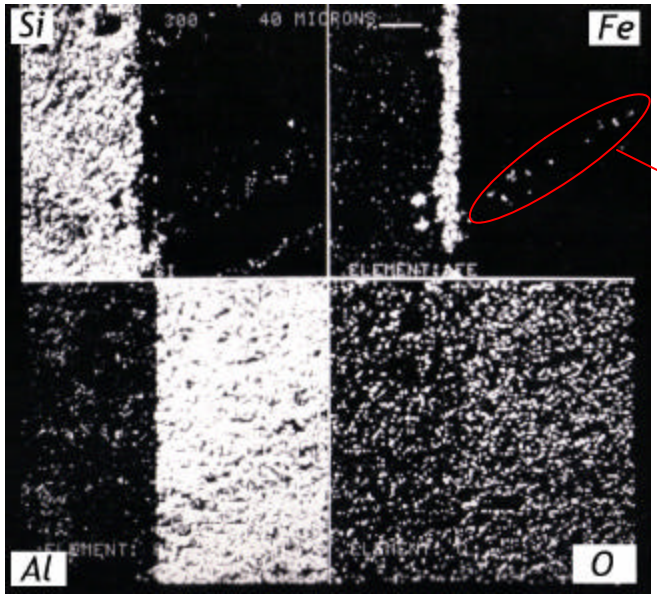

Figure 4-4- EDX scan of sapphire- coal slag interface after corrosion at 1200°C for 2 days (LEFT: coal slag, RIGHT: sapphire)

Figure 4-5 presents the sapphire samples corroded in coal slag at 1200°C over 3 days. This micrograph displays apparent interfaces on both sides. On the top sides of the sapphire samples, the microstructure of the coal can be noticed. On the bottom, the coal spalled off the sample and the side of the sample can be seen.

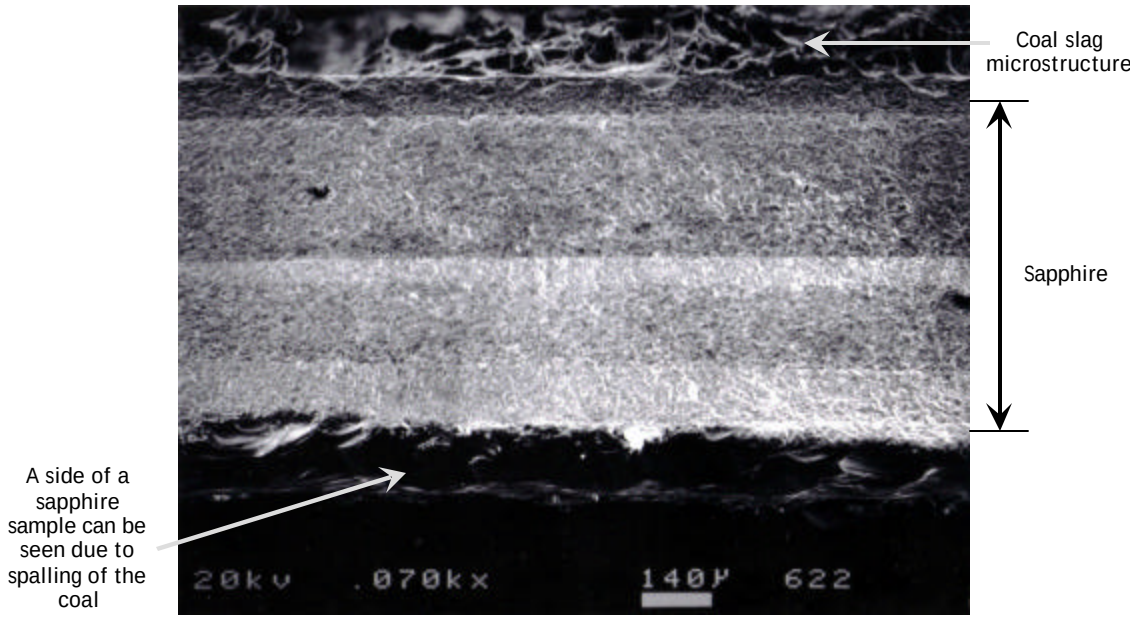

Figure 4-5- SEM micrograph of sapphire corrode in coal slag at 1200^{o}C for 3 days

Under the conditions of 1200^{o}C over 4 day period, the sapphire again showed no dramatic changes in the interface, Figure 4-6. Yellow highlights identify the interfaces between the sapphire and the coal slag. Both interfaces are strait with no major defects.

Figure 4-6- SEM micrograph of sapphire corrode in coal slag at 1200°C for 4 days

Figure 4-7 represents the SEM micrograph for the sapphire sample which was corroded in coal slag at the temperature of 1300°C for 2 days. Similarly to the previous micrographs, this sample exhibits high corrosion resistance, no degradation and no indications of an interfacial reaction product. However, this sample of completely spalled from the coal slag, and both of its sides are being exposed in this picture. They appear white on the micrograph due most likely to charging effects in the SEM, as labeled.

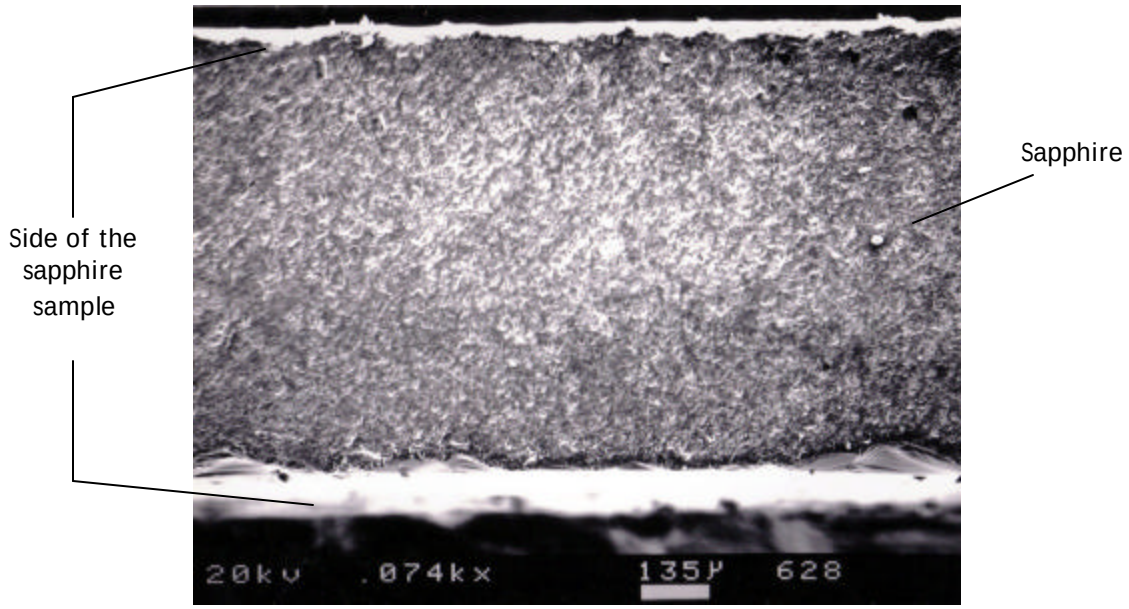

Figure 4-7- SEM micrograph of sapphire corrode in coal slag at 1300°C for 2

The following two micrographs do not obtain any significant microstructural features, but do show intense cracking of the sapphire samples (Figure 4-8 and Figure 4-9). Since the strength of the sapphire is largely dependant on its surface finish quality, any micro scale damages can be responsible for this mechanical failure at high temperatures. The strength of sapphire samples can be significantly improved by appropriate polishing. Sapphire plates used for corrosion experiments on this work were highly polished. The only unpolished parts were the thickness sides of the samples that were cut with diamond saw. Although those sides were very small in comparison with front and back surface, it is possible that imperfections in them caused sapphire samples to crack under the conditions of high temperature and corrosive slags.

Figure 4-8 shows severe damages in the surface of the cross sectional cut from the sapphire sample that underwent heat treatment at 1300^{o}C for 3 days in the corrosive coal slag. The left interface is hard to distinguish because of the large crack, but the right interface shows no deviations from the observations in the previous micrographs.

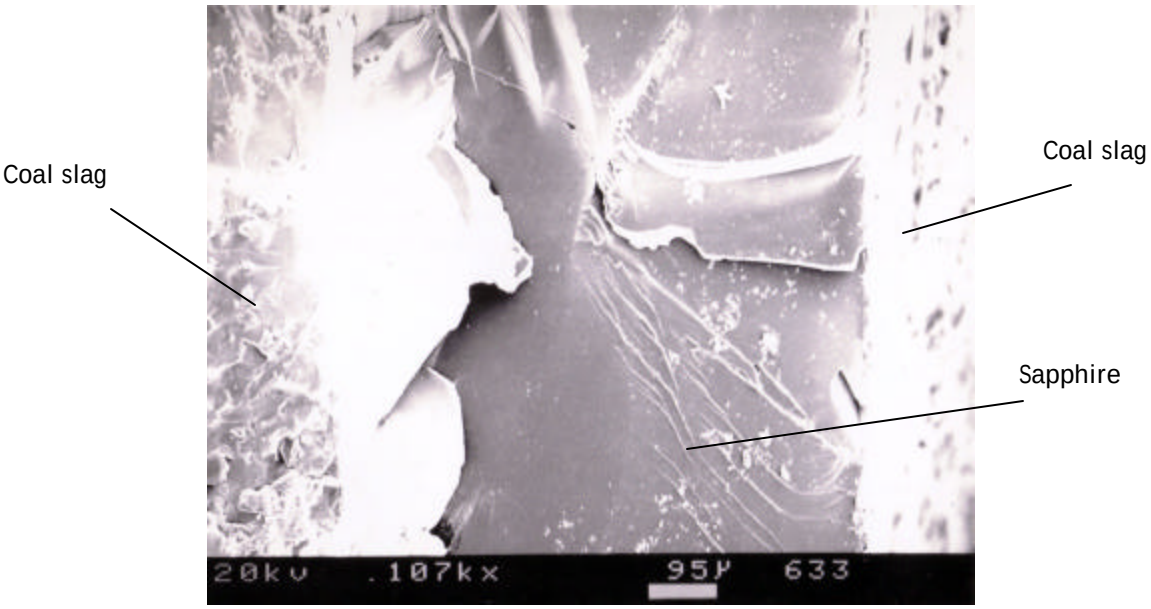

Figure 4-8- SEM micrograph of sapphire corrode in coal slag at 1300^{o}C for 3 days

Despite the large fractures, Figure 4-9 demonstrates that sapphire resists the attack of the corrosive coal slag even after experiencing cracking. This cracking originated from high thermal shocks during the heating and cooling process. The top interface had damage, but the bottom interface shows the strait line between the sapphire sample and the coal slag.

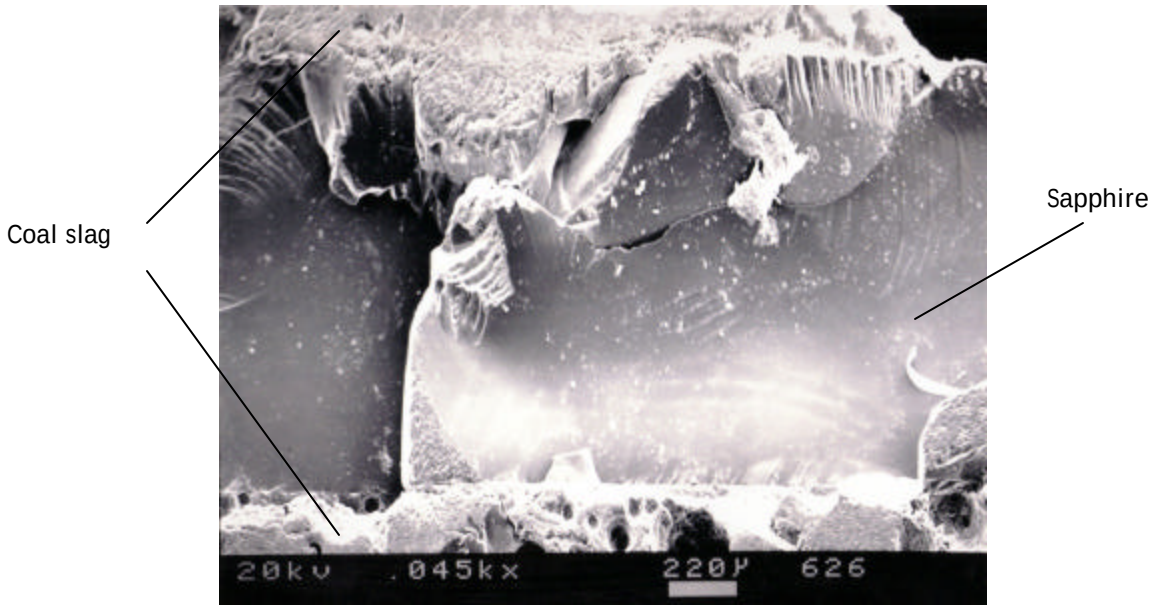

Figure 4-9- SEM micrograph of sapphire corrode in coal slag at 1300°C for 3 days

Figure 4-10 shows another interesting observation. Iron did not segregate at the sapphire interface, but to the surfaces of the gas bubbles within the slag. This may lead to the conclusion that iron is diffusing towards any free surface. This conclusion can also apply to the previous EDX scans that reveal iron segregation at the sapphire surface (Figure 4-3 and Figure 4-4). It is possible that the coal slag spalled of the sapphire during corrosion and that there was a free surface where the iron diffused to. It is also possible that the iron preferentially segregates to the sapphire slag interface due to a lowering of the overall energy of the system with the occurrence of this phenomenon. The remark of iron crystals in M. K. Ferber's and V. J. Tennery's work[13] can be of particular interest to our work, since we observed similar iron segregation in coals slag.

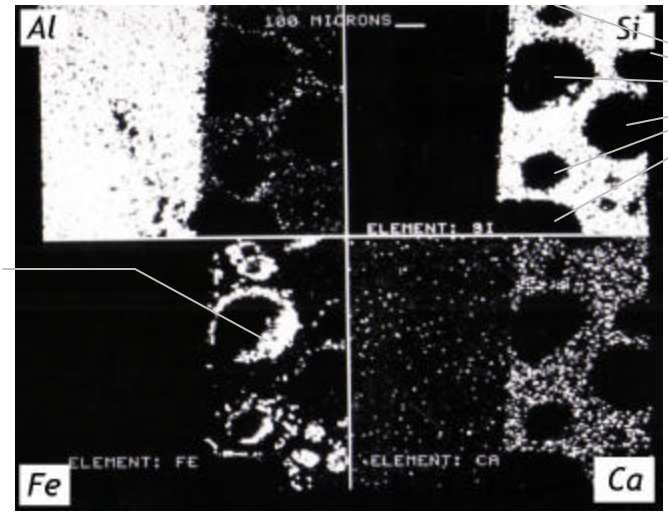

Figure 4-10- EDX scan of sapphire- coal slag interface after corrosion at 1300°C for 4 days (LEFT: sapphire, RIGHT: coal slag)

Lastly, the most severe condition for sapphire corrosion tests was conducted at 1400°C for 4 days.

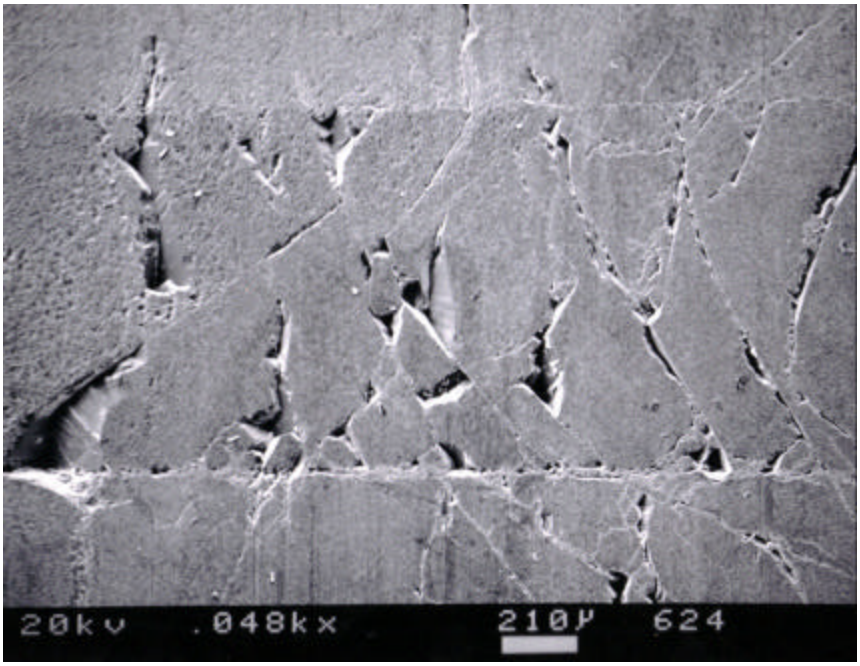

Figure 4-11- SEM micrograph of sapphire corroded in coal slag at 1400°C for 4 days

4.1.2. Sapphire in Soda Lime

The difficulties of removing soda lime glass from the samples are mentioned in Section 3.6 and discussed in detail in Section 4.4. Due to these difficulties, it took much longer time to obtain the thickness measurements for sapphire and zirconia in soda lime glass.

4.1.2.1 Thickness Data

The thickness data presented in Table 4-2- Change in thickness of sapphire in soda lime glass shows very small corrosion amounts for 1200°C and 1300°C. The data points obtained for 1200°C show no apparent trend. However, the data gathered for 1300°C slightly increases as the time exposure in the glass at this temperature increases. This can best be seen in Figure 4-12.

Table 4-2- Change in thickness of sapphire in soda lime glass

Days in furnace	1200°C	1300°C	1400°C
1	0.06	0.03	0.04
2	0.04	0.05	
3	0.03	0.07	
4	0.03	0.11	

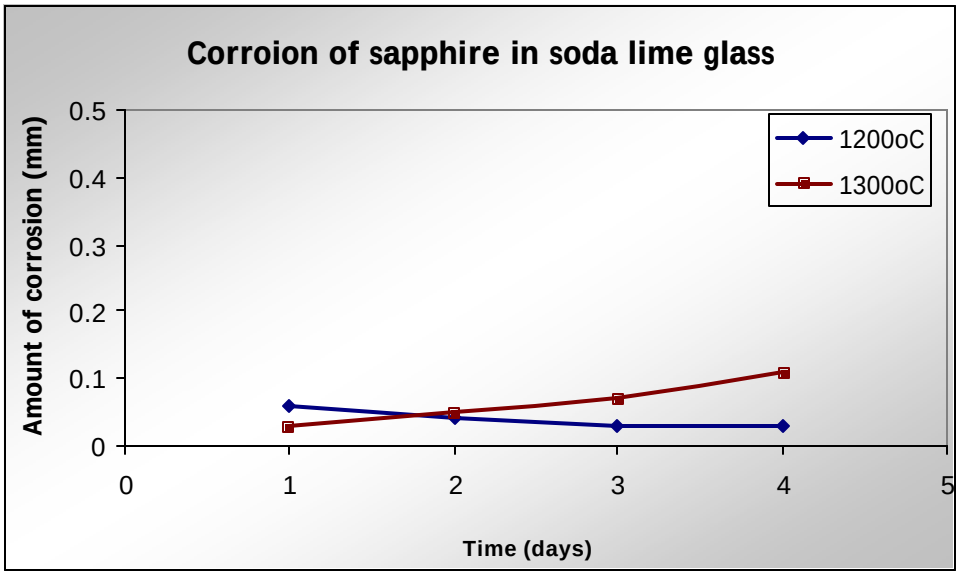

Figure 4-12- Amount of corrosion versus reaction time and temperature for single crystal sapphire in soda lime glass

4.1.2.2 Surface and interface analysis

The sapphire- soda lime interfaces appear clear with no suggestion of interfacial product formation or degradation due to corrosion. Sapphire samples in soda lime glass also exhibit less cracking than in coal slag. Spalling however occurred in the soda lime environment as well.

Figure 4-13 represents the interface between the sapphire sample and the soda lime glass after the corrosion experiment was conducted at 1200^{o}C for 1 day, which was the mildest corrosion condition. The bottom interface shows a uniform spalling crack along the sample surface. The top interface is barely visible due to absolutely any effect of the high temperature glass exposure. The white areas on the sapphire sample on the micrograph are due to charging which occurs as a result of insufficient coating of the sample with gold.

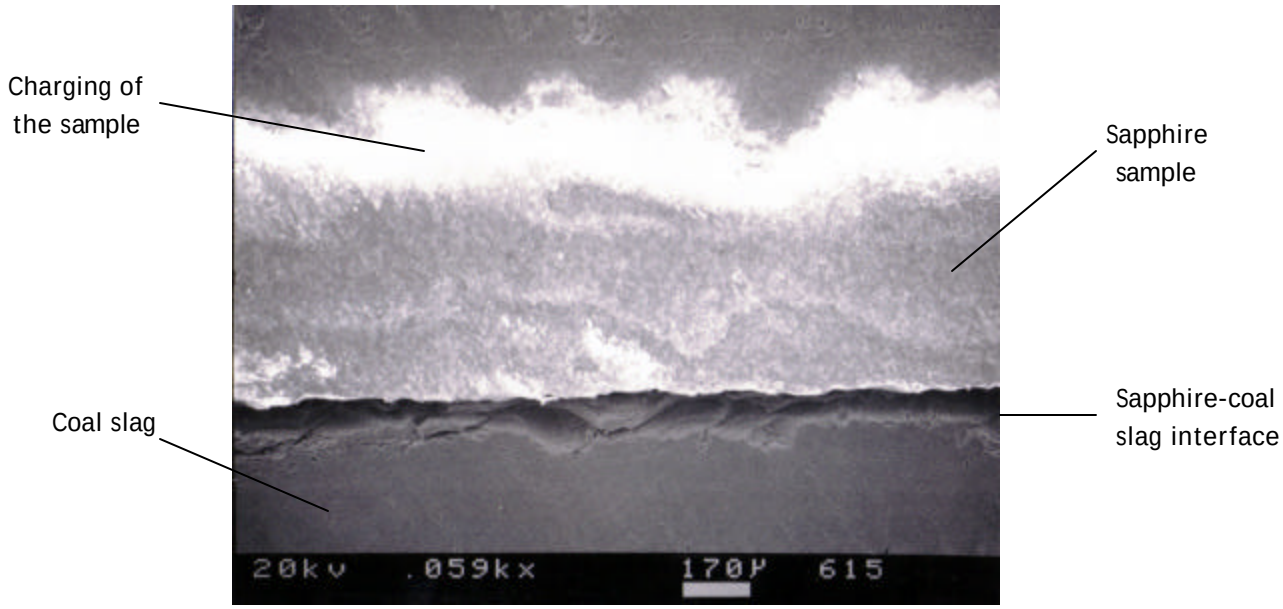

Figure 4-13- SEM micrograph of sapphire corrode in soda lime glass at 1200°C for 1 day

Figure 4-14 reveals a complete separation of the sapphire sample from the soda lime glass most likely due to spalling. There are visible scratches on this sample that come from cutting with diamond saw.

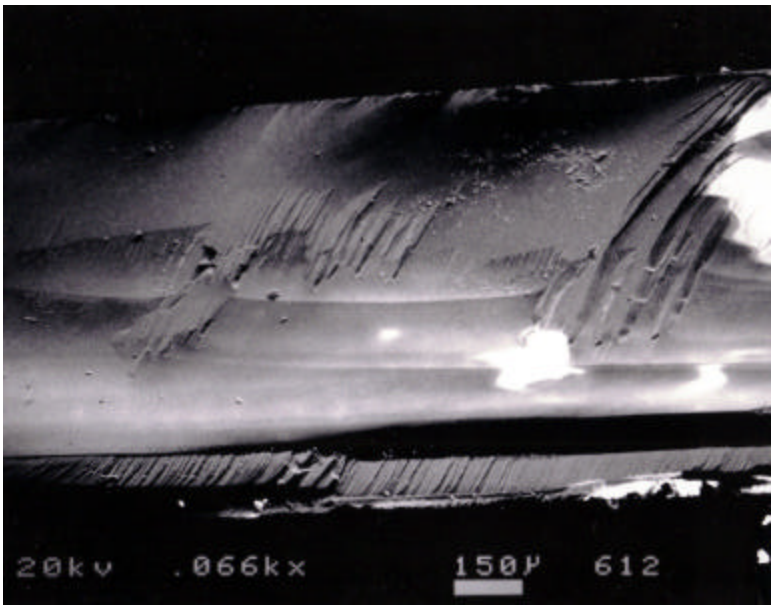

Figure 4-14- SEM micrograph of sapphire corrode in soda lime glass at 1200°C for 2 days

Figure 4-15 is another good example of corrosion resistance of sapphire in soda lime glass. After the treatment at 1200°C for 3 days, this sample shows neither degradation nor cracking. There are some imperfections at the bottom interface, which can be a result of the cutting. The top interface shows some cracks in the glass and its separations from the sapphire.

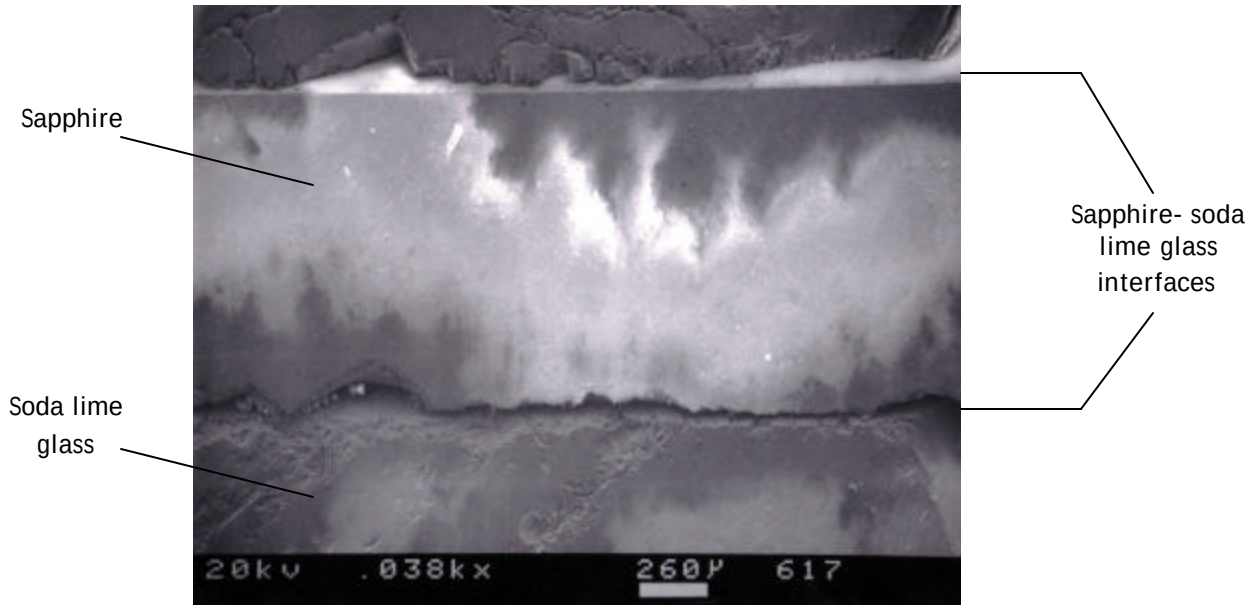

Figure 4-15- SEM micrograph of sapphire corrode in soda lime glass at 1200°C for 3 days

After the 4 days of corrosion treatment of the sapphire in the soda lime glass at 1200°C, there are some microstructural features at the interface that can be addressed (Figure 4-16). While the top interface shows no change on the sapphire side, and only expected spalling of the glass, the bottom interface shows a region where a possible change in microstructure or grain growth may have occurred. There is still a clear interface line between the sample and the glass.

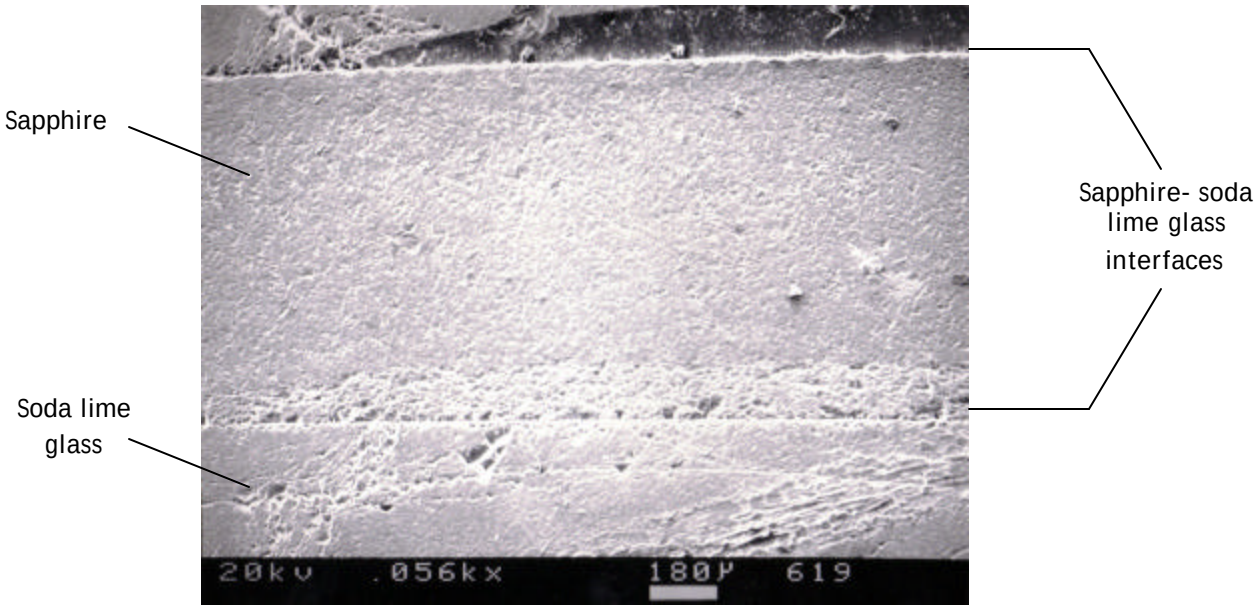

Figure 4-16- SEM micrograph of sapphire corrode in soda lime glass at 1200°C for 4 days

Figure 4-17 represents a sapphire sample that was corroded in soda lime glass for 1 day at 1300°C. This SEM micrograph is not a good illustration of the corrosion effects at the interface because of its apparent stigmatism effect. Yet, this figure shows another example of complete spalling of sapphire away from the glass.

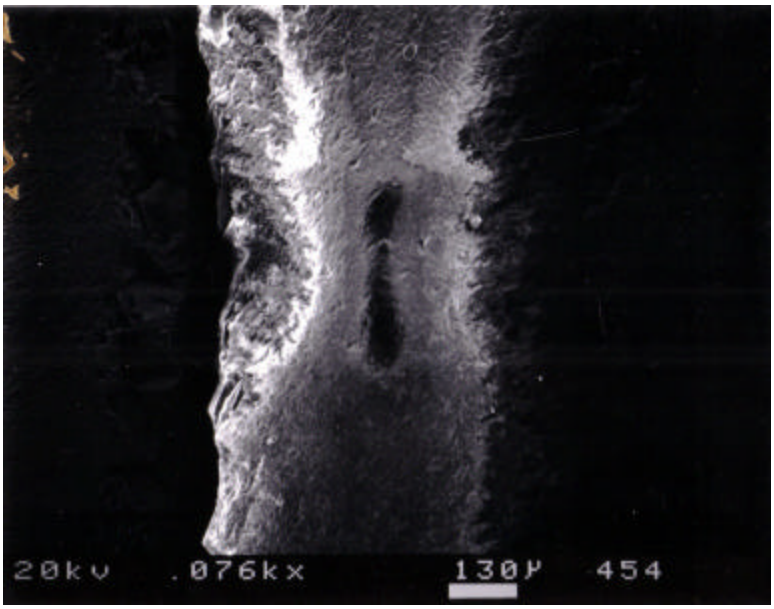

Figure 4-17- SEM micrograph of sapphire corrode in soda lime glass at 1300°C for 1 day

When scanning for elements in the soda lime glass, aluminum, silicon, calcium and sodium were the elements that are most abundant and therefore important to scan for. Sapphire in soda lime slag exhibited straight and clear interfaces that indicate no signs of formation of the interface product as seen in Figure 4-18.

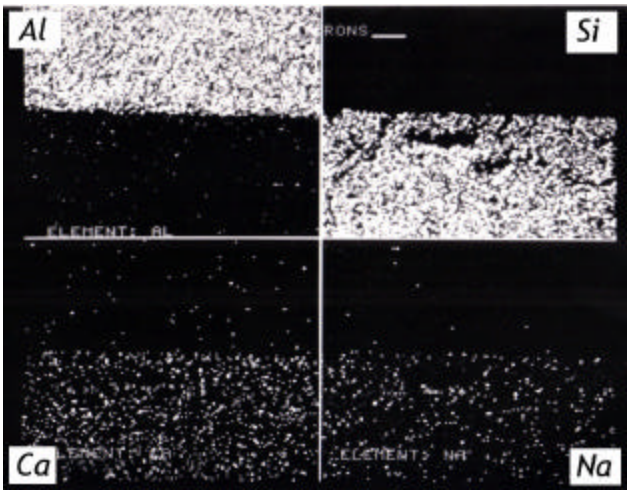

Figure 4-18- EDX scan of sapphire- soda lime glass interface after corrosion at 1300°C for 1 day (Top: sapphire, BOTTOM: soda lime glass)

Figure 4-19 represents an SEM micrograph of sapphire corroded in soda lime at 1300°C for 2 days. This micrograph shows evidence of stigmatism due to the SEM: the sample is distorted and appears to be narrower in the middle than at the ends. Intense charging is also observes near the top interface.

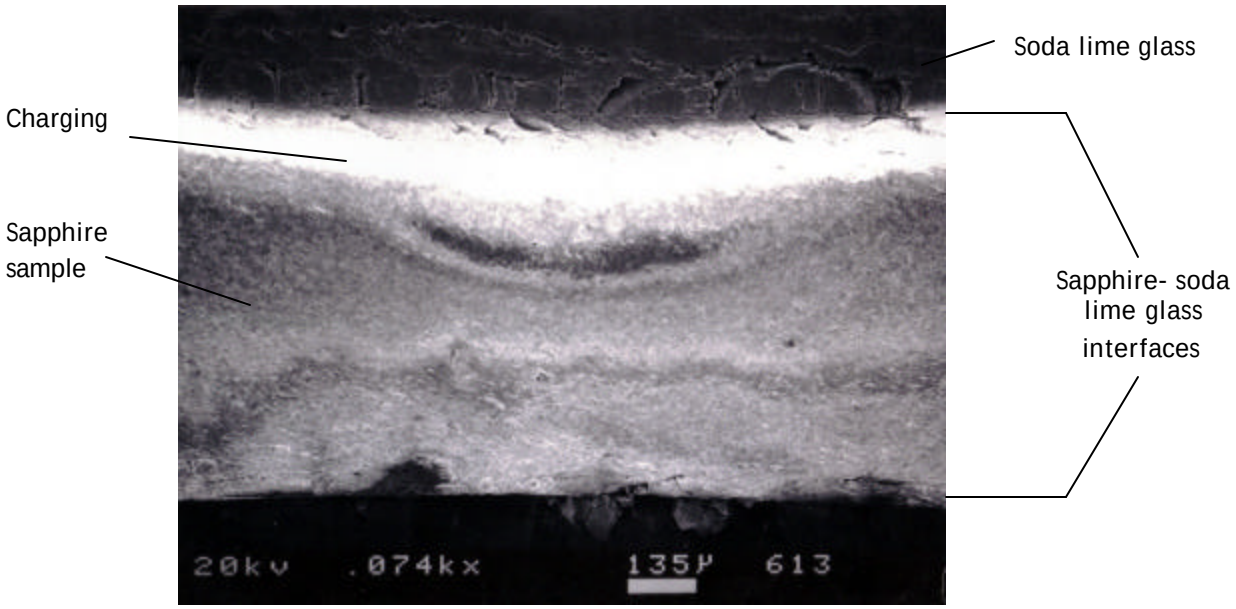

Figure 4-19- SEM micrograph of sapphire corrode in soda lime glass at 1300°C for 2 days

Figure 4-20 represents the SEM micrograph of sapphire in soda lime glass corroded for 3 days at 1300°C. There are numerous microcracks on the glass side, although the sapphire side of the interface displays no signs of corrosion effects. The right side of the sapphire sample is completely separated from the glass, and consequently, the side of the sapphire sample can be observed in this micrograph. It appears as a white strip because it was not coated and therefore it exhibits some charging.

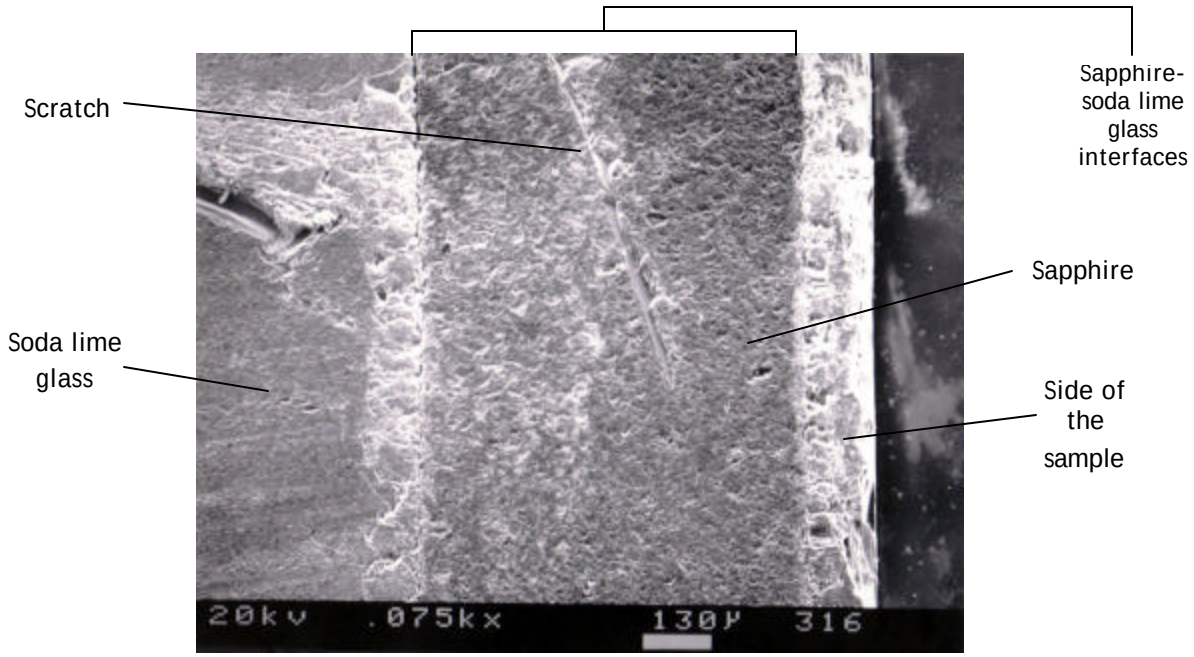

Figure 4-20- SEM micrograph of sapphire corrode in soda lime glass at 1300°C for 3 days

To examine whether there is formation of an interfacial product, elemental analysis of the interfacial area was performed. A series of elemental spot scans was obtained to follow any changes in elemental composition that might take place. To closely examine the interfacial elemental composition it is necessary to scan for elements on both sides of the interface as well as at the interface. Therefore three scans were acquired. Figure 4-21 shows the elemental examination of the spot on soda lime glass next to the interface with sapphire. Naturally, the elements presented on this scan are the ones found on soda lime glass: silicon (most abundant), aluminum, sodium and calcium. Comparing this scan to the scan of soda lime glass (Figure 3-2), there are no obvious differences in relative amounts of elements present. Hence, it can be concluded that there is no diffusion of elements towards the interface and there is no existence of any products forming at the glass side of the interface.

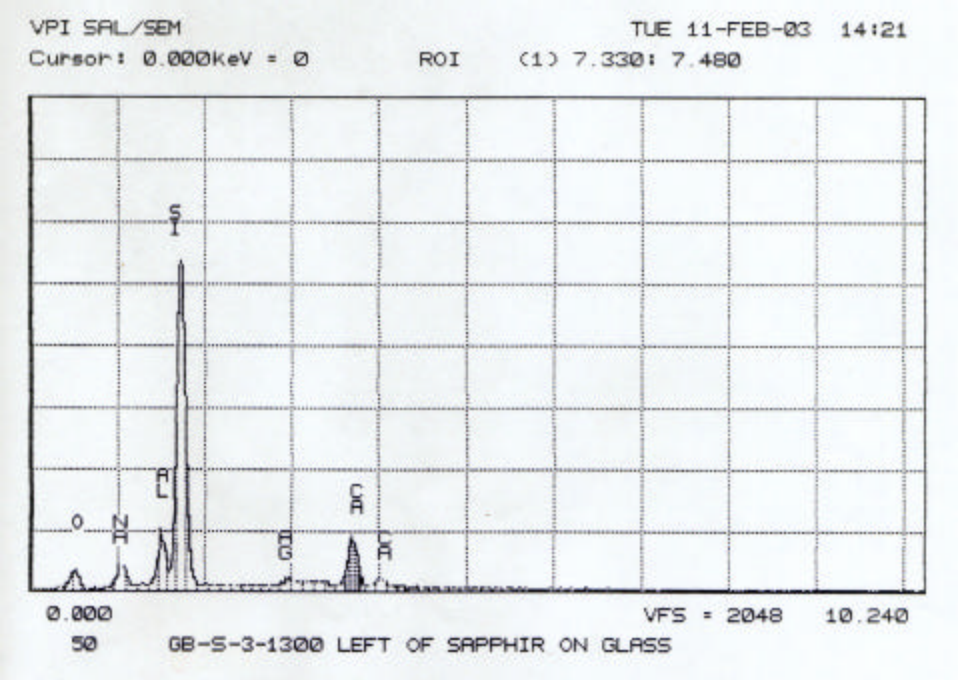

Figure 4-21- elemental scan a spot on soda lime glass next to the interface with sapphire

The elemental scan of the spot which lies on the interface of sapphire and soda lime glass, shown in Figure 4-22, illustrates the existence of elements from both sapphire (alumina) and soda lime glass (silicon, alumina, sodium and calcium). The only feature that this scan differs from the pervious one is in relative amount of aluminum compared to other elements in the scan. Therefore, the only logical interpretation of it is that it contains the elements from materials from both sides of the interface and since sapphire is aluminum oxide, the relative intensity of the aluminum peak will be greater than that in Figure 4-21.

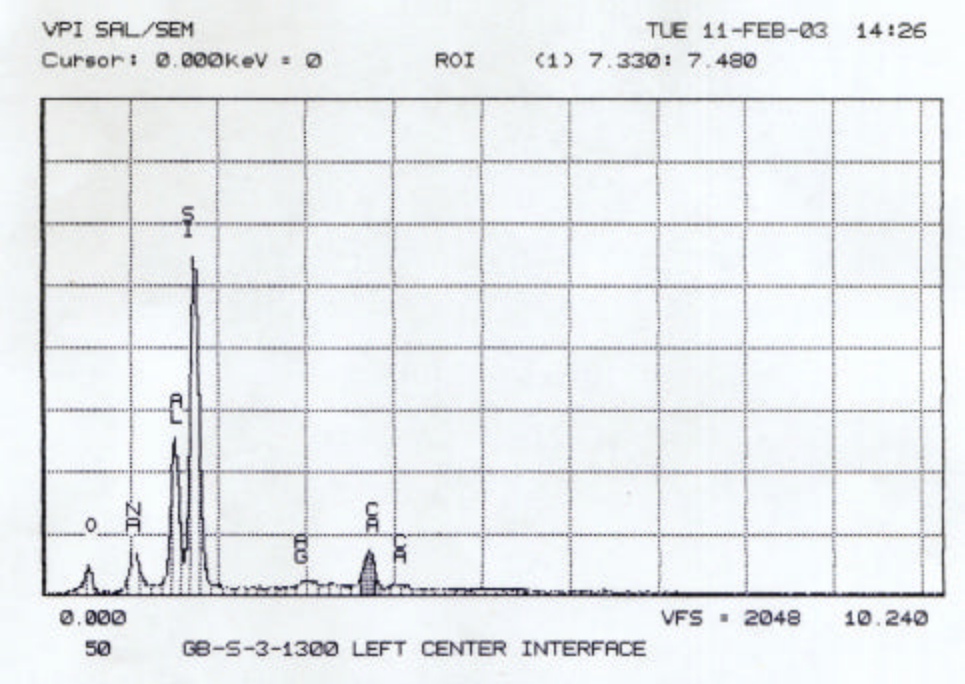

Figure 4-22- elemental scan of a stop on the sapphire- soda lime interface

Lastly, the elemental composition of a spot inside the sapphire sample was obtained. As expected, only aluminum and oxygen peaks are identified, as they are the only elements that are contained in sapphire. The silver peak comes from coating material used in the SEM sample preparation.

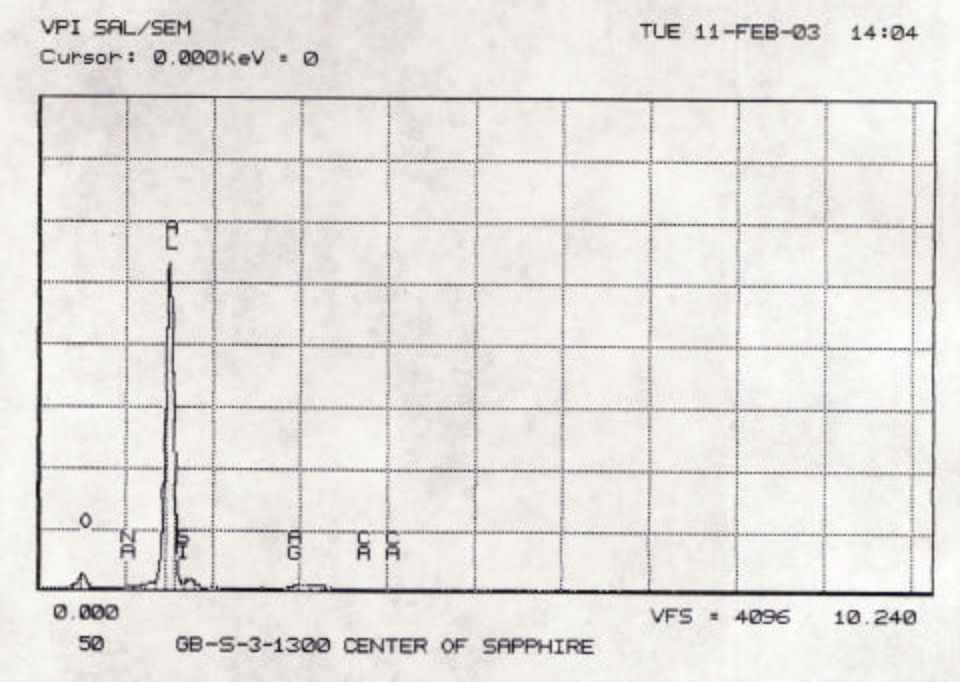

Figure 4-23- elemental scan of a spot inside the sapphire

After a corrosion treatment for 4 days at 1300^{o}C, Figure 4-24, the sapphire sample showed some microstructural changes due to corrosion in the soda lime glass. Both interfaces exhibit intense cracking. It also appears this cracking is on the glass side of the interface, bus has combined together with the sapphire. This micrograph might suggest the existence of some interfacial product formation on sapphire in soda lime glass.

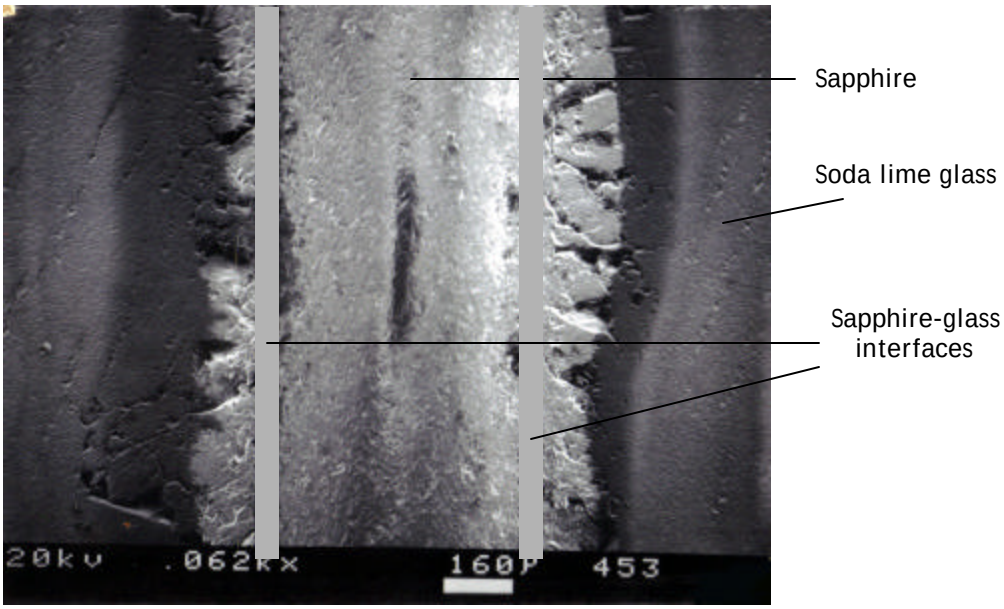

Figure 4-24- SEM micrograph of sapphire corrode in soda lime glass at 1300°C for 4 days

4.2 Zirconia

The corrosion of zirconia was conducted through similar experiments as for sapphire. Zirconia was corroded in coal slag and soda lime glass at high temperature and for different times. The amount of corrosion was obtained from the difference between the final and initial thickness measurements. Zirconia was cut into samples using a diamond saw and those samples were not further processed before the heat treatment. The zirconia samples showed much more intense cracking and spalling than sapphire under the same conditions. It is possible that the severe cracking and spalling in the zirconia samples was caused by flaws that were introduced by cutting.

Due to such an intense cracking of the zirconia samples, very few thickness measurements were possible. It is possible that the stabilizing agent was depleted which caused the cubic zirconia to transform to tetragonal or

monoclinic. The mechanical strength of monoclinic phase of zirconia is drastically less than that of cubic phase. Similar observations were noted in work done by V. K. Pavlovkii, Yu. S. Sobolev[25] and M. Yoshimura, T. Hiuga and S. Somiya[21]. In most cases these pieces were so small that any thickness measurements were impossible. The samples that had good enough size for thickness measurements broke when subjected to polishing with alumina sand paper. As a result of the mentioned complications, the data points do not carry as much confidence as the sapphire data.

4.2.1. Zirconia in Coal Slag

Zirconia samples in coal slag experienced more cracking than in the glass. In countless cases, after the slag was removed, the samples separated into very small pieces that were impossible to measure accurately for thickness with the calipers. Due to extreme difficulties of conducting corrosion experiments with zirconia samples, there are very few data points obtained.

4.2.1.1 Thickness Data

The three corrosion amounts obtained of zirconia samples in coal slag are presented in Table 43. The much greater values for corrosion amounts compared to sapphire in the same coal slag may be explained by zirconia decomposition into monoclinic phase in such corrosive environments and under high temperatures, as discussed in Section 2.2.

Table 4-3- Change in thickness of zirconia in soda lime glass

Days in furnace	*1200°C*	*1300°C*
1		0.132
2	0.059	
3		0.59
4		

4.2.1.2 Surface and interface analysis

Figure 4-25 shows the intense spalling of the zirconia in the coal slag after only one day at 1200°C. The coal slag seems to be attached to the zirconia on the bottom interface and spalling occurs around this part of the slag from the bulk slag. The presence of numerous gas bubbles can be seen in this picture.

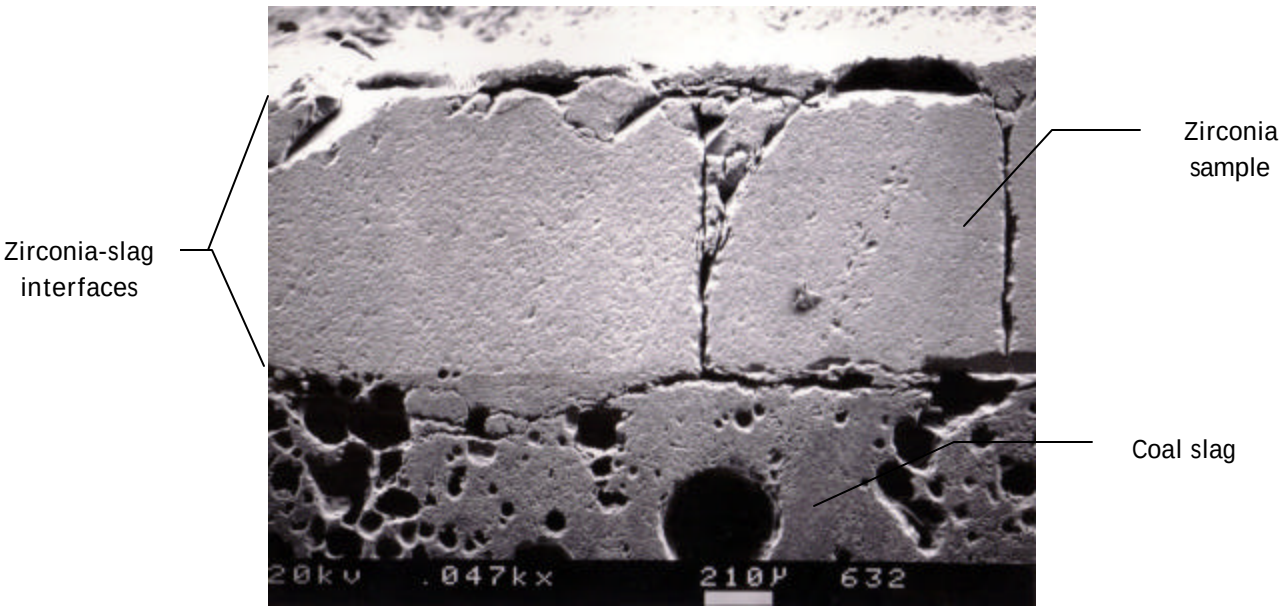

Figure 4-25- SEM micrograph of zirconia corroded in coal slag at 1200°C for 1 day

The EDX scan of zirconia in coal slag, Figure 4-26, shows distinct interfaces between the zirconia sample and the slag, which indicates no

degradation of the sample. As the literature suggests, Section 2.2, corrosive slags may have effect other than dissolution of the yttria stabilized zirconia. As a result of being exposed to the slag constituents, yttria stabilized cubic zirconia may undergo phase transformation to monoclinic, which is a likely reason for intense cracking. This EDX scan does not demonstrate any significant reaction of the zirconia sample taking place, but this does not exclude the possibility of phase transformation occurring as a consequence of exposure to the corrosive slag at high temperature. Calcium dots show on both zirconia side and glass side. This does not mean that there is penetration of calcium into zirconia, but that the zirconia content in soda lime glass is so small that the computer image compensates for it by showing the relative concentrations of calcium in zirconia and glass. Since glass has very little calcium content and zirconia has none, the computer shows similar concentration of Ca dots on both sides. It only shows the relative amounts of Ca in zirconia to glass and not relative to other elements scanned. Similar phenomenon was also noted in Figure 4-3 and Figure 4-10.

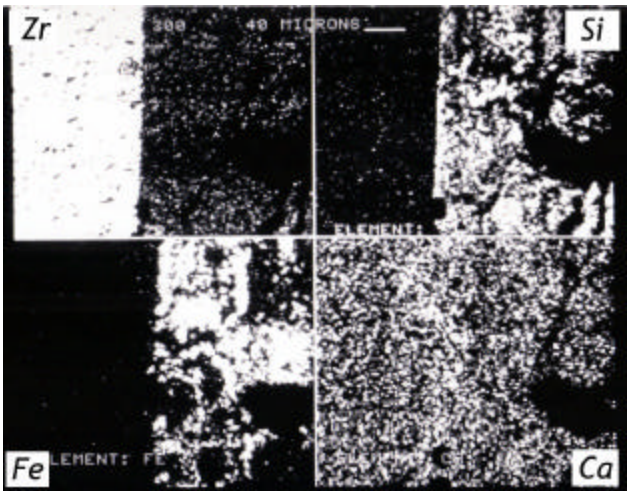

Figure 4-26- EDX scan of zirconia- coal slag interface after corrosion at 1200°C for 1 day (LEFT: zirconia, RIGHT: coal slag)

Figure 4-27 represents part of the zirconia sample in coal slag that is crack free. The coal slag in this sample had too many air bubbles around the interface and seems to be almost completely separated from the zirconia. Bright spots on the sample are believed to be the result of charging due to insufficient coating of the silver in the sputtering chamber. Also, the zirconia interface appears to have lots of micro-cracks and defects, which can best be seen on the right interface of Figure 4-27.

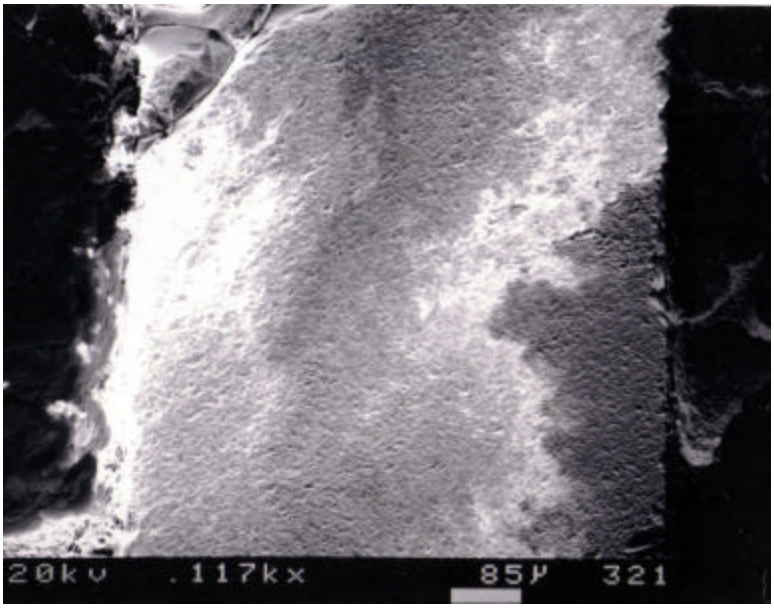

Figure 4-27- SEM micrograph of zirconia corroded in coal slag at 1200°C for 2 days

Another way to test for the presence of an interfacial reaction product is spot scans. A spot exactly at the interface between the zirconia and the coal slag was examined and elemental analysis performed by EDX, Figure 4-28. Comparing this scan to the scan of the coal slag, Figure 3-1, it can be concluded that both elements from coal slag and zirconia are present. Another interesting but not an unusual feature can be seen from this figure: the ratio of silicon to iron is different from that in Figure 3-1. The observation of

separation of silicon from iron in the coal slag and the segregation of iron to the interface of the sample in EDX scans was common. Hence, the ratio of silicon to iron changes from spot to spot. The importance of Figure 4-28 is to show that at a point which lies exactly at the interface between zirconia and coal slag, there is both materials present as it is expected when there is no formation of the interfacial product.

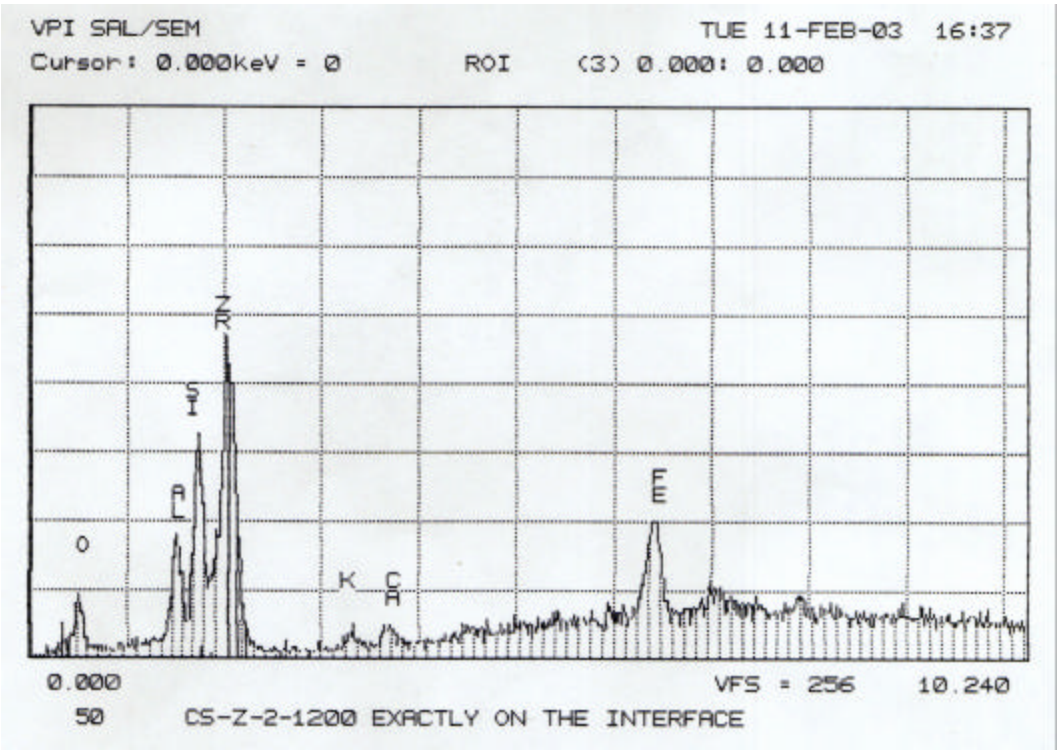

Figure 4-28- spot scan elemental analysis of the interface between zirconia and coal slag after 2 days of heat treatment at 1200°C

To further investigate if there is a product forming at the interface, another scan was obtained for the spot on zirconia right next to the interface, Figure 4-29. This scan shows that there is mostly zirconia present. There are traces of iron and calcium. Considering the relative amounts of iron and calcium compared to zirconium and even gold from coating, those traces are

most likely due to smearing during the cutting of the sample and not due to existence of the interfacial product.

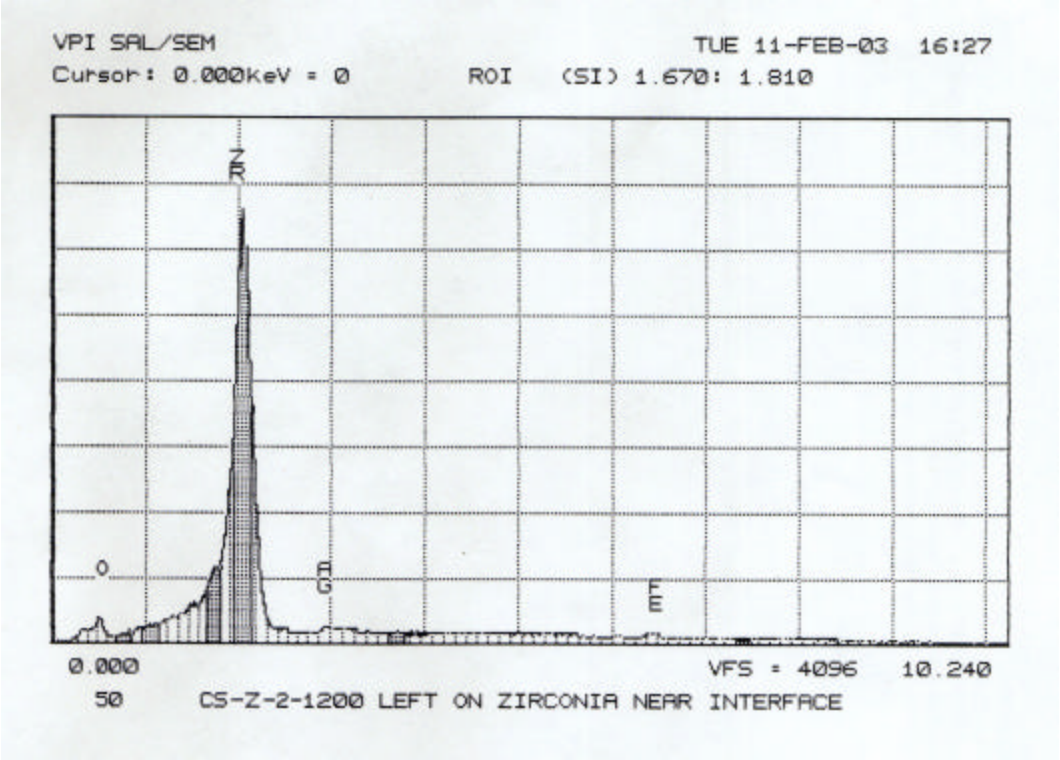

Figure 4-29- Spot scan elemental analysis of zirconia's side of the interface with coal slag after 2 days of heat treatment at 1200°C

The following four SEM micrographs, Figure 4-30, Figure 4-31, Figure 4-32, and Figure 4-33, represent zirconia in coal slag at 1300°C that was corroded for 1, 2, 3, and 4 days consecutively. All four micrographs reveal severe cracking within the zirconia samples. It can also be noticed from those micrographs that there is no coal slag around the samples. This is due to spalling of zirconia from the slag after the heat treatment and cutting of the samples. Although there is no evidence of the formation of the interfacial product, there seems to be a change in the mechanical strength of the zirconia. This change in mechanical strength can be interpreted from evidence in the literature on zirconia, Section 2.2 where many authors have experienced

the phase transformation in zirconia from tetragonal or cubic to monoclinic. It may be that due to this change, the zirconia samples were easily broken into very small pieces, and since those pieces were even smaller than the thickness of the sample, the measurements were impossible to conduct.

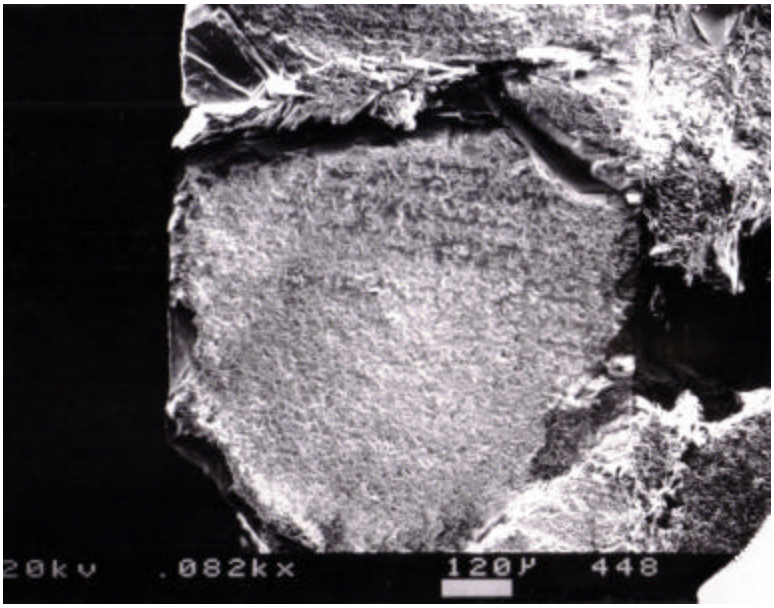

Figure 4-30- SEM micrograph of zirconia corroded in coal slag at 1300°C for 1 day

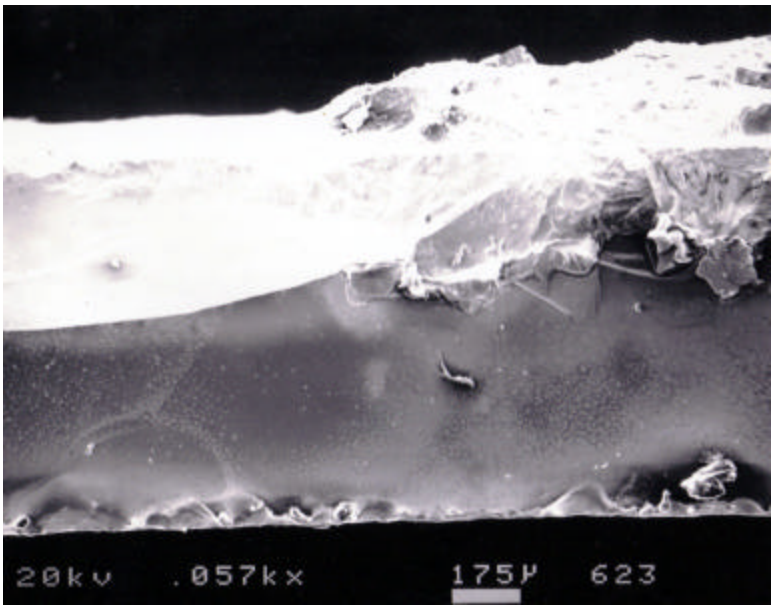

Figure 4-31- SEM micrograph of zirconia corroded in coal slag at 1300°C for 2 days

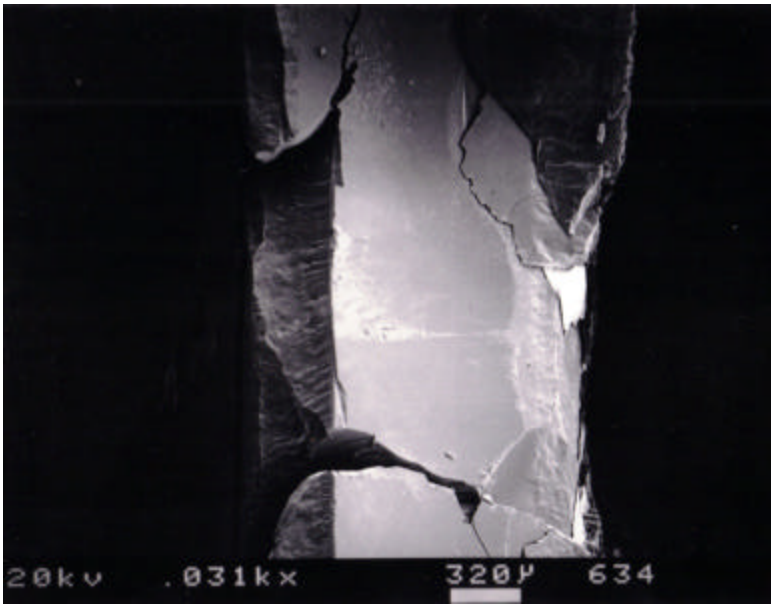

Figure 4-32- SEM micrograph of zirconia corroded in coal slag at 1300°C for 3 days

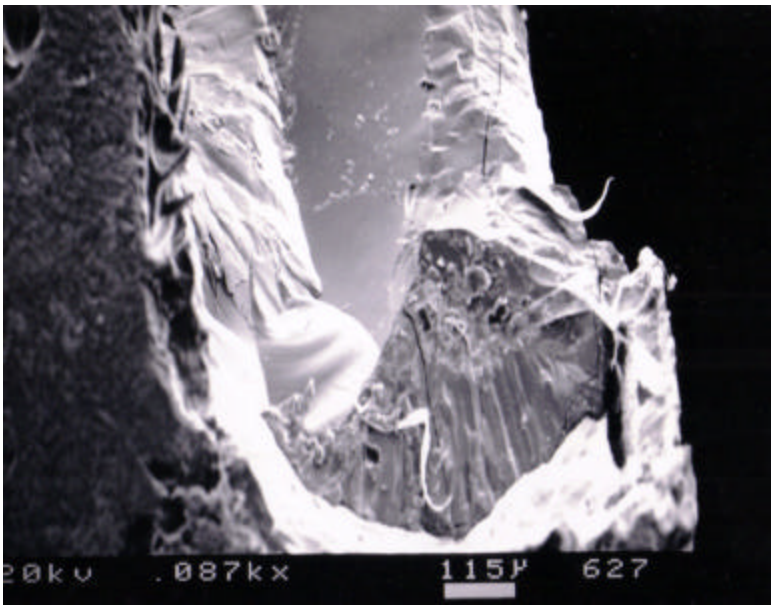

Figure 4-33- SEM micrograph of zirconia corroded in coal slag at 1300°C for 4 days

4.2.2. Zirconia in Soda Lime Glass Slag

The observations in corrosion experiments of zirconia in soda lime glass followed in similar fashion as zirconia in coal slag. The thickness measurements were difficult to conduct. However, the SEM micrographs showed distinct interfaces with no spalling at all. Experiments in soda lime melts generally had less spalling than in coal slag.

4.2.2.1 Thickness Data

As already discussed previously, the data collection for zirconia was difficult due to cracking and breaking of the samples into pieces that were too small to measure. For this reason, only a few data points were possible to obtain, Table 4-4. It is very likely that the data points are not good representatives of the corrosion process of single crystal fully stabilized cubic zirconia in soda lime glass. It is possible that the samples that were measured

were even chipped and that the different between the final and the initial thicknesses was caused by the chipping of the samples and not by their corrosion. For example, the data obtained for zirconia in soda lime slag at 1300°C that was reacted for 3 days shows the degradation of zirconia sample of 0.344mm. Since neither the SEM micrograph (Figure 4-40) nor the EDX scan (Figure 4-44) show images that present corrosion taking place, there is a great possibility this data point is incorrect. Perhaps the thickness measurements were obtained from a broken sample.

Table 4-4- Change in thickness of zirconia in soda lime slag

Days in furnace	*1200°C*	*1300°C*
1	0.05	0.14
2	0.09	
3		0.344
4		

4.2.2.2 Surface and interface analysis

The zirconia-soda lime interface did not show the formation of an interfacial reaction product when analyzed by SEM. The interfaces were smooth and clear with no observation of spalling.

Figure 4-34, Figure 4-35, and Figure 4-36 present zirconia samples corroded in soda lime glass at 1200°C for 1, 2, and 3 days consecutively. All three micrographs display a uniform interface of zirconia in soda lime glass at this high temperature. Strait and smooth interfaces with no spalling indicate neither degradation nor formation of the interfacial product. The white areas on those micrographs illustrate charging of the sample inside the SEM chamber.

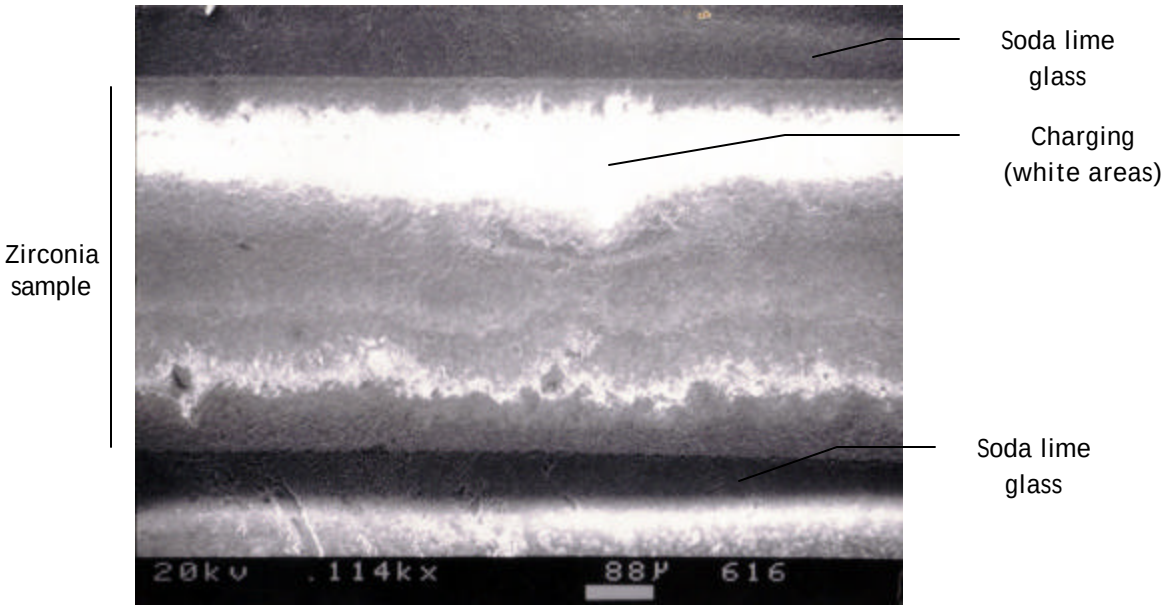

Figure 4-34- SEM micrograph of zirconia corroded in soda lime glass at 1200°C for 1 day

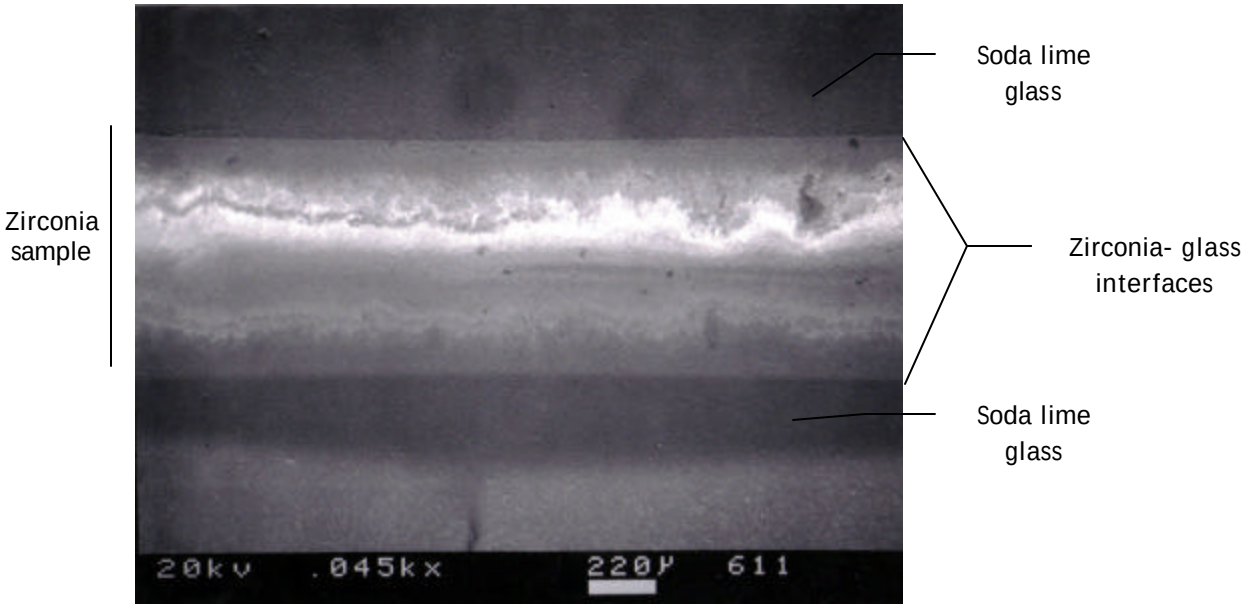

Figure 4-35- SEM micrograph of zirconia corroded in soda lime glass at 1200°C for 2 days

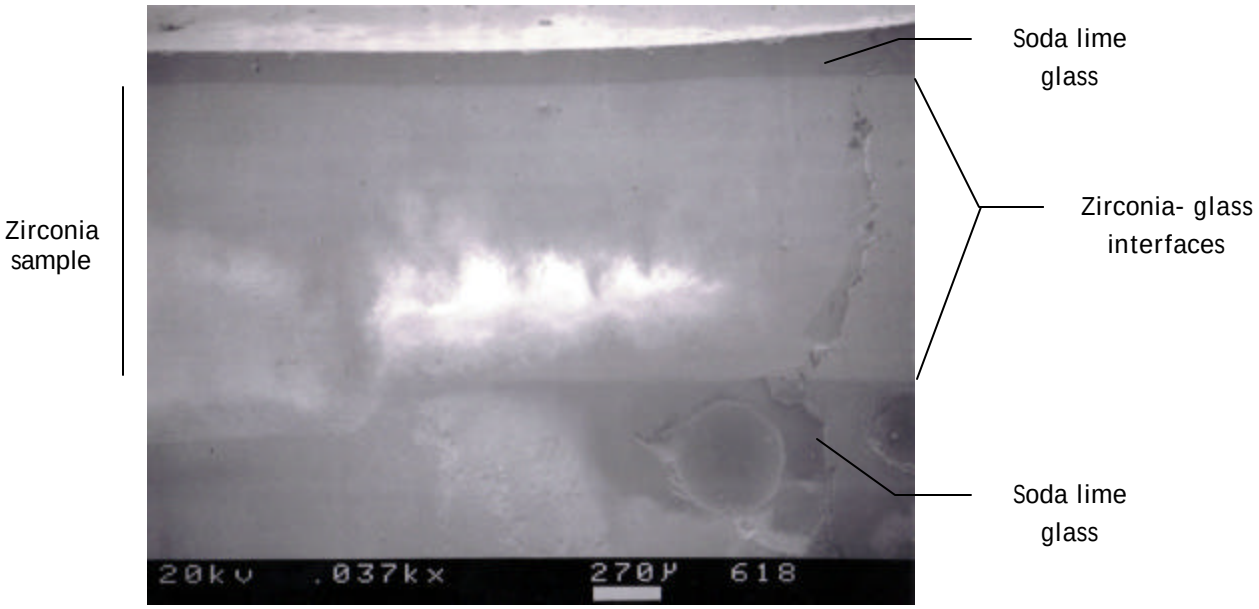

Figure 4-36- SEM micrograph of zirconia corroded in soda lime glass at 1200°C for 3 days

After 4 days at 1200°C in soda lime glass, zirconia experienced some microcracks along the interface. Even so, the sample snows no degradation.

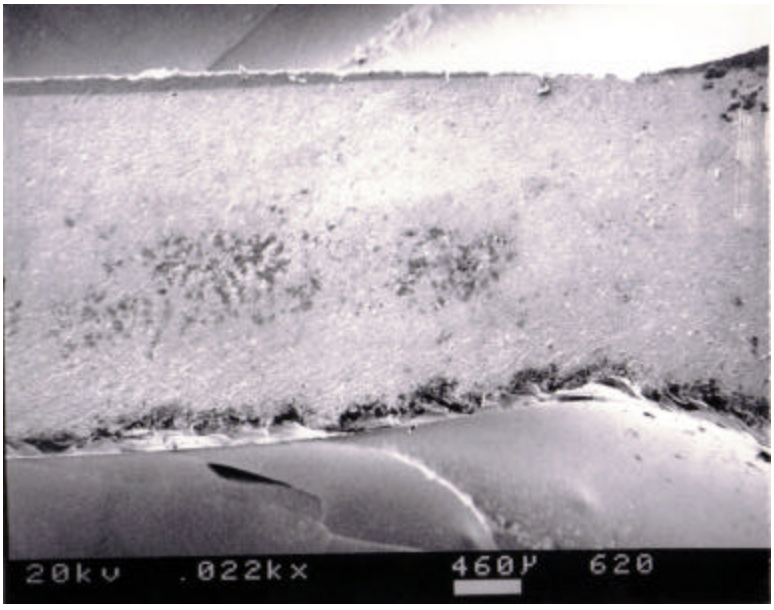

Figure 4-37- SEM micrograph of zirconia corroded in soda lime glass at 1200°C for 4 days

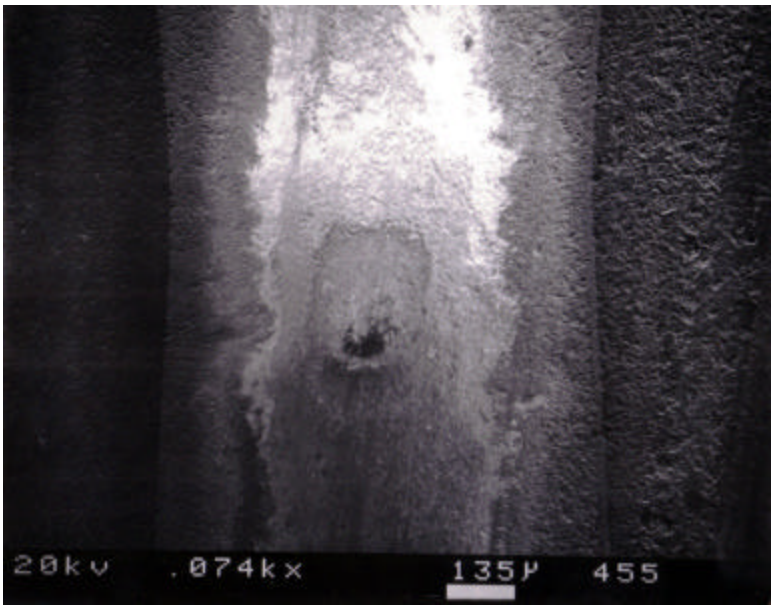

Figure 4-38- SEM micrograph of zirconia corroded in soda lime glass at 1300°C for 1 day

Figure 4-39 and Figure 4-40 represent samples of zirconia corroded in soda lime glass at 1300°C for 2 and 3 days consecutively. Both of these micrographs appear to have double interface lines on both sides which possibly indicates the formation of the interface product layer.

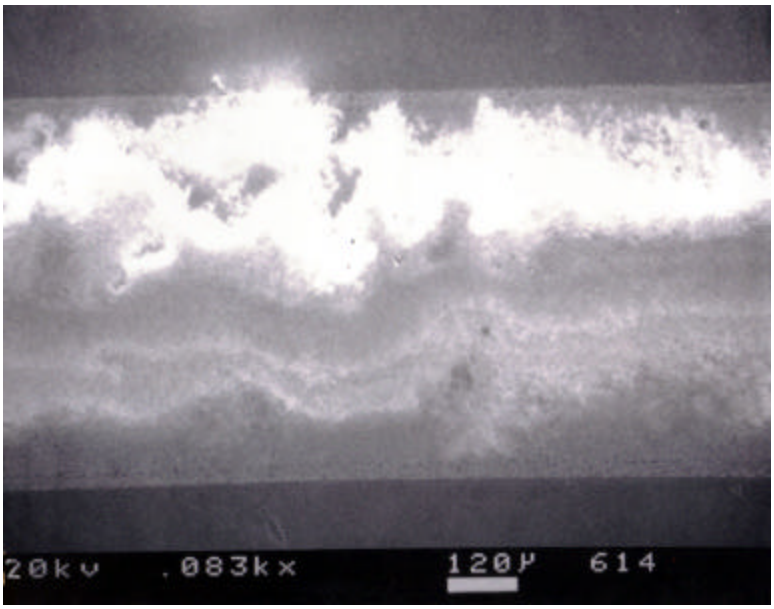

Figure 4-39- SEM micrograph of zirconia corroded in soda lime glass at 1300°C for 2 days

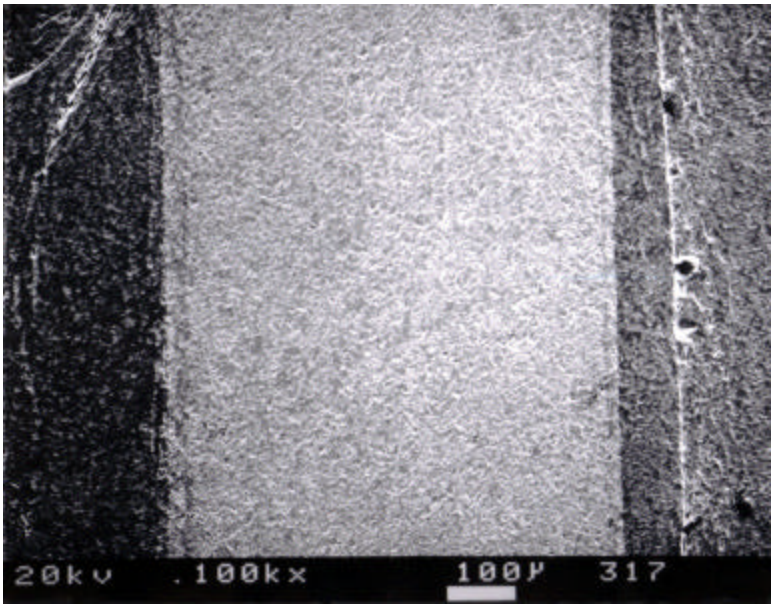

Figure 4-40- SEM micrograph of zirconia corroded in soda lime glass at 1300°C for 3 days

The further interface analysis of the zirconia sample which was corroded in soda lime glass at 1300°C for 3 days was performed by obtaining the elemental spot scans. From the information obtained from those scans, it can

be interpreted as if there is neither interfacial product formation nor degradation of the zirconia sample due to corrosion.

Scanning for the elemental composition on the glass side next to the zirconia-soda lime glass interface, it is evident that there is no other product than soda lime glass itself. The peaks on this scan closely resemble ones in the soda lime scan in Figure 3-2. The exception of the small shoulder peak of zirconium can be noted as well. The small zirconium peak is probably the result of smearing during the slicing of the sample with diamond saw. The dust from the sample generated by the saw during cutting fills the microcracks in the glass and may be detected in this scan.

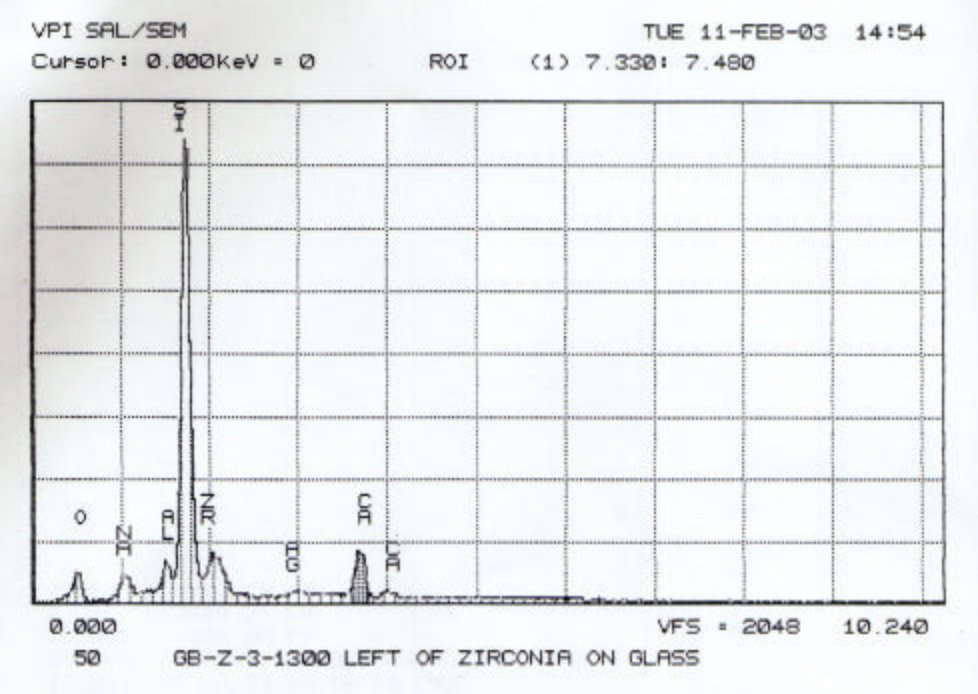

Figure 4-41- Elemental scan of the spot on soda lime glass next to the interface with zirconia

Figure 4-42 displays an elemental scan of the spot on zirconia next to the interface with soda lime glass. The zirconium peak is far more prominent

that the other peaks. The silicon peak arising from the shoulder of zirconium peak is most likely due to saw smearing.

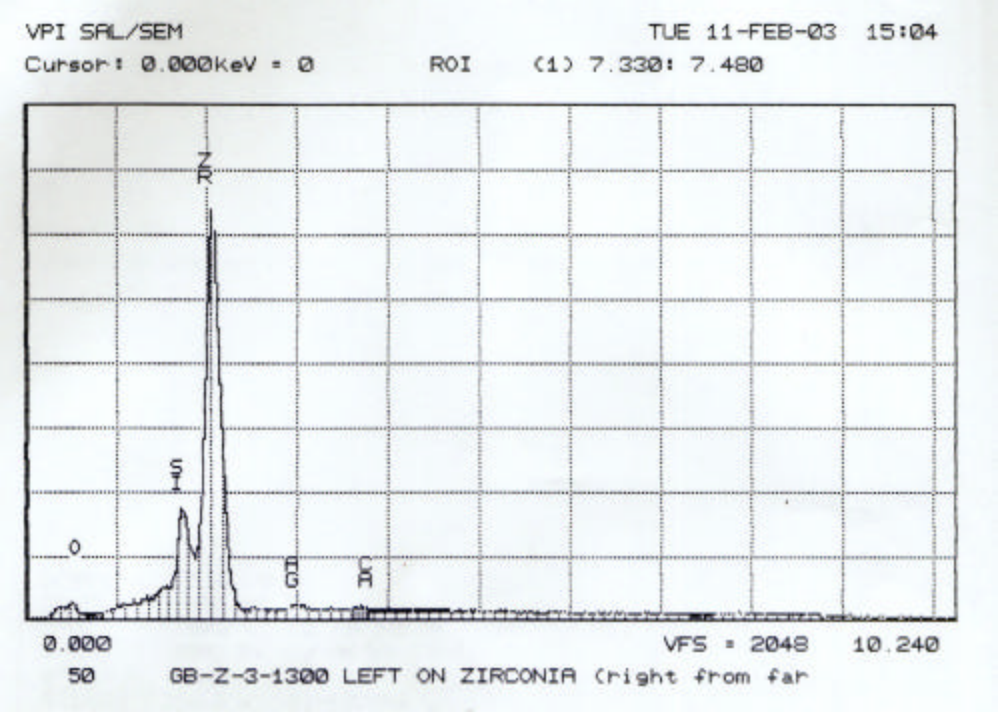

Figure 4-42- Elemental scan of the spot on zirconia next to the interface with soda lime glass

Figure 4-43 represents an elemental analysis of the zirconia sample that was corroded in soda lime glass at 1300^{o}C for 3 days. This scan indicates that the sample consists purely of zirconia. The silicon shoulder peak is again probably the result of smearing with the saw during cutting the cross sectional slides out of the sample.

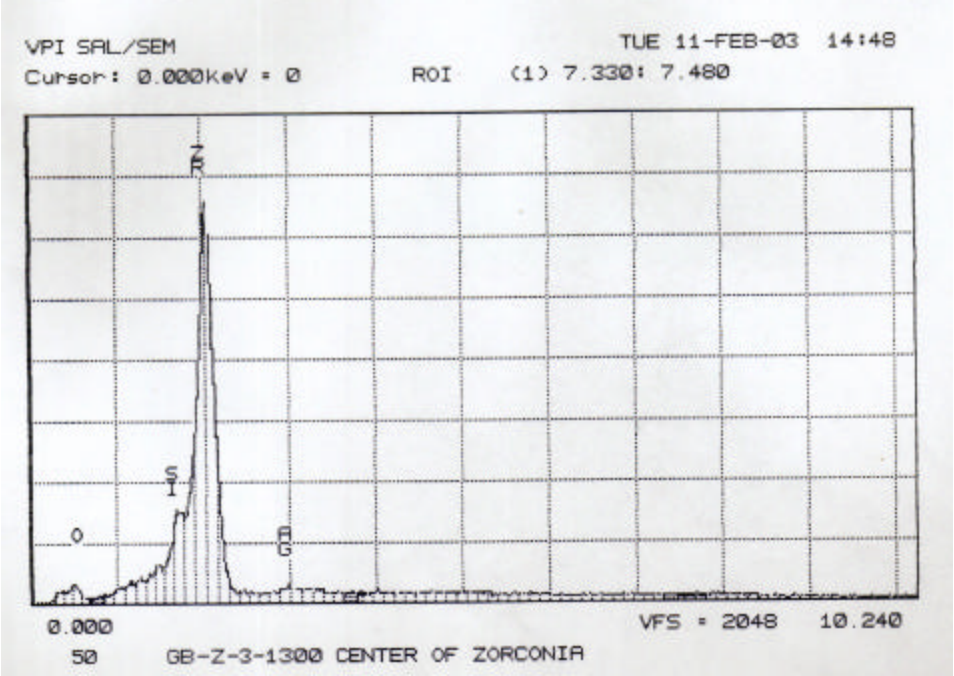

Figure 4-43- Elemental scan of the spot on zirconia sample

The importance of the spot scans of zirconia in soda lime glass is that the interpretation of the data can result in the conclusion that neither interfacial product nor diffusion of any elements towards or away from the interface has occurred. The comparison of the spot scans of soda lime glass (Figure 3-2) and zirconia (Figure 4-43) with the spot scans of both glass and zirconia side of the interface (Figure 4-21 and Figure 4-22 consecutively) reveals no change in the relative amounts of the elements.

The EDS elemental scan of this sample indicated no formation of the interfacial product. The concentration of all four elements scanned does not change near the interface.

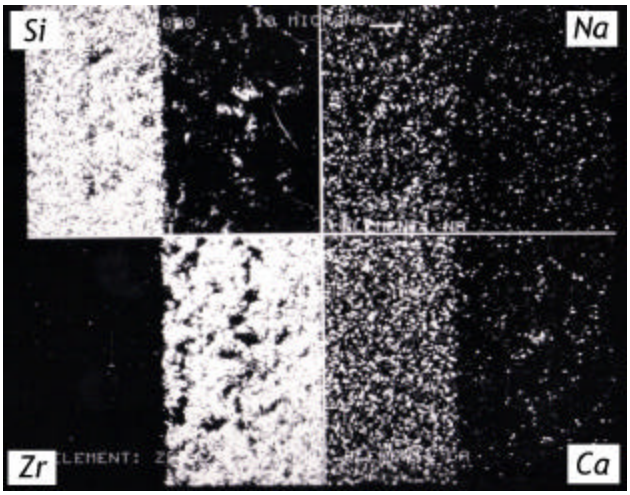

Figure 4-44- EDX scan of zirconia- soda lime glass interface after corrosion at 1300°C for 3 days (LEFT: soda lime, RIGHT: zirconia)

After a 4 day treatment at 1300°C in soda lime glass, the zirconia micrograph shows similar observation to those for the 2 and 3 days exposure times (Figure 4-39 and Figure 4-40).

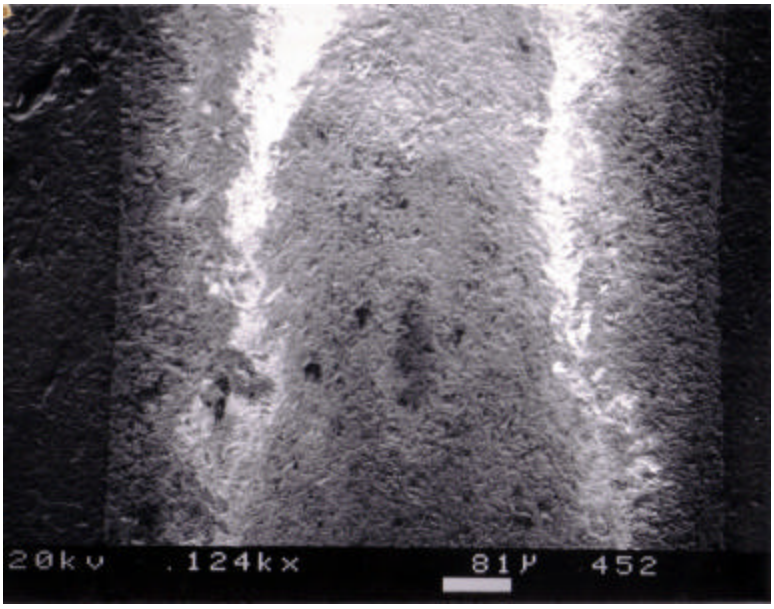

Figure 4-45- SEM micrograph of zirconia corroded in soda lime glass at 1300°C for 4 days

The thickness of zirconia samples was very difficult to measure due to severe cracking that zirconia experienced as a result of mismatch in the thermal expansion coefficient coefficients. After the heat treatments, zirconia samples not only split into many smaller pieces, but all those pieces also separated from the coal medium. This observation may lead to the conclusion that the main corrosion mechanism in zirconia occurs through spalling.

4.3 Activation Energies

The dependence of corrosion on temperature can be expressed by the Arrhenius equation:

$$j = A\exp(E_c / RT)$$

where j is the rate coefficient, A is a constant, E_c is activation energy, R is the universal gas constant, and T is the temperature in degrees Kelvin[27]. The Arrhenius equation shows that the dependence of corrosion on temperature and is expressed in terms of activation energy, E_c. Based on the data in Table-1, it is difficult to obtain the value of the activation energy. A large range of values makes this calculation impossible. Corrosion of sapphire and zirconia in the soda lime and the coal slag cannot be interpreted in terms of a single activation energy. The reason for this may be constant change in the composition of slag around the sample and therefore the change in driving force for diffusion[12]. In addition, there are many additional factors which may influence this– bubble formation influencing the amount of corrosion, very small thickness changes making measurement inaccuracy more significant, and segregation of iron to the interface. Since the slag composition varies with temperature and time, the corrosion mechanism and rate controlling step may change as well. The possibility of having multiple corrosion mechanisms taking place in the same reaction is large. Those mechanisms might change depending

on temperature, fluidity of the slag, or saturation of the boundary layer with alumina or zirconia.

4.4 Error Analysis

The variations in thickness data which follows no apparent trends may indicate the existence of many sources of errors. The errors associated with experiments and thickness measurements are explained in detail in the following sections.

4.4.1. Difficulties with HF Treatment

Hydrofluoric acid worked better on dissolving coal slag than soda lime glass. Soda lime took a long time to dissolve, sometimes up to two months. HF reacts with soda lime forming a white product on the outside which is soft and brittle and can easily be removed by sand paper. The sample would then be placed back into the HF and another layer of white product would be formed and removed, and so on.

For zirconia in soda lime and coal slag environments, especially at higher temperatures (1400^{o}C), after the glass or slag was dissolved, the samples would separate into very small pieces, almost like a dust, that made thickness measurements difficult. This is most likely due to destabilization of the cubic phase back to monoclinic phase of the zirconia sample. It may be that during the cooling process, forces caused by the difference in thermal expansion coefficient of the sample and of its environment were exerted on the sample causing it to crack. Since the monoclinic phase of zirconia is mechanically unstable, fracturing is certain when forces are exerted. The sample would still be held together by the solidified environment, but once this environment is

dissolved off with HF, the sample would fall into pieces. In the cases where these pieces were bigger than 1mm, it was still possible to take measurements. At higher temperatures, especially 1400^{o}C, cracking was more intense and many samples had to be heat treated to be able to obtain some measurable pieces after dissolving the glass or slag material in HF. This problem was more intense with zirconia than with sapphire. This problem added to other difficulties of obtaining the data for zirconia, which gave a large standard deviation and challenging interpretation of data.

To minimize this problem of cracking during the cooling from 1400^{o}C to room temperature, the cooling rate was decreased as low as 2 degrees per minute. Unfortunately, this effort did not minimize the cracking. To further confront this problem, another approach was carried out. Before the heat treatment, a sample of sapphire or zirconia was attached to the tip of a silica rod (about 3mm in diameter) with alumina cement to the shorter end. After the cement dried, the rod with a sample attached to it was inserted into the Deltech furnace from the top through an opening of about 6mm in diameter so that the sample was placed inside the crucible. After the appropriate amount of heat treatment, the rod with the sample was lifted above the crucible and left inside the furnace while it cooled. In this manner, the amount of slag left on the sample would be small enough, relative to the sample, which was expected to drastically decrease the cracking. Unfortunately, another problem emerged from this method. The parts of the silica rods that were inside the furnace deformed during heating making it difficult to pull up. Often they cracked allowing the samples to fall back inside the slag.

4.4.2 SEM Method Induced Errors

Since the interfaces of all samples were well defined in general, this method was expected to work well. Pictures obtained from the SEM were clear and measurements were easily obtained. Unfortunately, a large source of error was identified. The samples were tilted and rotated at an unknown angle inside the crucible so that the cut was not perpendicular to the sample and therefore the thickness obtained was larger than the "real" thickness by an unknown percentage. Upon calculating the angle the real thickness was obtained (Table 4-1). This angle was calculated by measuring the positions of the top and bottom of the sample relative to crucible base according the Figure 4-46. Once the angle is known, it can be used to calculate the sample thickness:

$$\text{True thickness} = \cos(\Theta) \times \text{Measured thickness}$$

where Θ is the angle at which the sample was tilted inside the crucible. Due to the complications of measuring the angle after various rotations inside the crucible during the heat treatment, the data obtained in this way was doubtful. This data was very different in some cases when compared to the data obtained by HF method for the same samples. For example for sapphire sample in coal slag that was corroded for 1 day at 1200^{o}C, the HF method gave the thickness of 0.75mm while SEM method gave 0.98mm. This large discrepancy is most likely due to inability to accurately measure the angle of the sample rotation during the heat treatment. For this reason, the SEM method of obtaining the final thickness of samples after corrosion was abandoned.

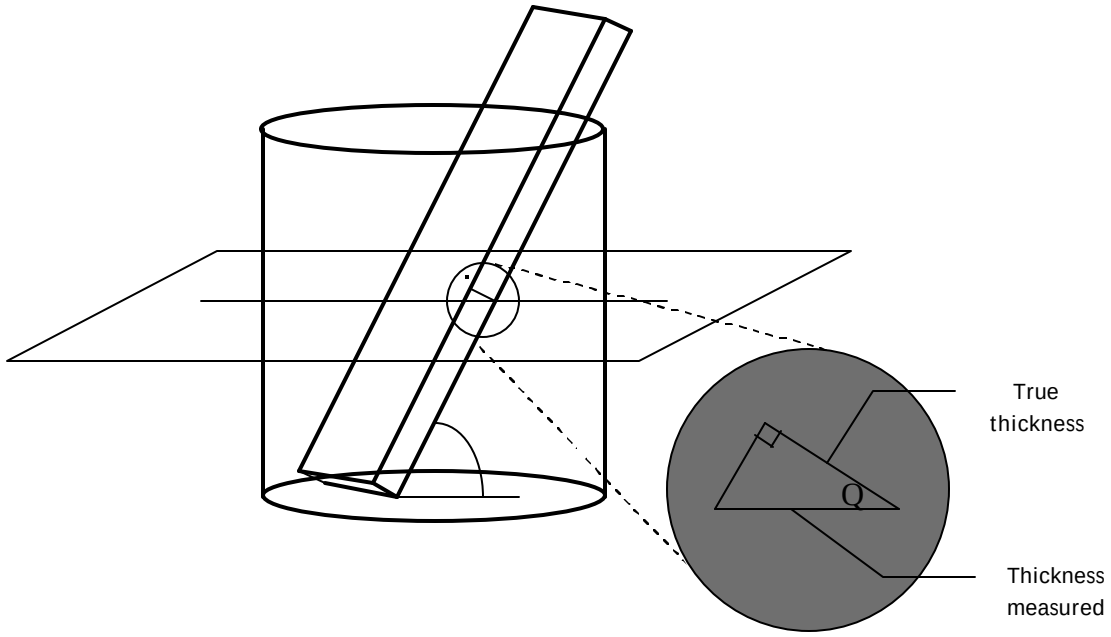

Figure 4-46-schematic representation of the angle at which the sample is tilted and then sliced inside the crucible

4.4.3 Sources of Errors due to Experimental Methods

It is important to note that the samples were not quenched after the heat treatment. The temperature was ramped down at rate of 5^{o}C/minute in order to minimize cracking due to difference in thermal expansion coefficient. The point at which the slag solidified around the sample could be different for every sample. Some SEM micrographs show the possibility of formation of an interfacial product, and some show no change in the sample, some measurements indicate degradation, and some show no change from initial thickness. Also, in general because of the difficulty and expense in running the samples, only one sample for each temperature and time was evaluated. There were no other values to compare the measurements with, and there was no averages taken among samples.

Since the sapphire and zirconia samples were cracked during the heat treatment, and after the dissolution of slag there was nothing to hold them together, very few measurable pieces were collected. Most of the pieces were too small- even smaller than the sample thickness of 0.8mm. Data shown in table k represents the average of all measurements taken on the sample. Not all the pieces of the sample were measured due to their small size, and therefore the result obtained is not the average of the whole sample, but the average of the measurable pieces of the sample. Some samples, especially zirconia at 1400^{o}C, were completely turned into dust except one small piece. In this case, the measurements were possible only on these pieces and they were averaged out.

Another important source of error is uneven corrosion. Because the slag bubbles at higher temperature, it overflows the crucible. Over the course of the reaction, the level of the slag slowly decreases causing bottom of the sample to corrode more. In many cases, the sample of sapphire and zirconia were broken into smaller pieces due to the mismatch in thermal expansion coefficient with the slag during the solidification process. During the dissolution of the slag by HF acid etching, the small pieces of the sample would mix together. When they were measured, it was unknown whether they came from the top or the bottom. In the cases where large thickness differences within one samples were measured and large standard deviation obtained, it was an indication of this phenomenon. In other cases where the measurements were not too far apart, it was an indication that only one part of the sample was measured and the average was taken only of that part not the whole sample.

There is another cause of uneven corrosion. A. R. Cooper Jr. and W. D. Kingery noted that more intense corrosion takes place immediately below and

above the slag surface due to surface forces[11]. This points the possibility that the data points that show greater corrosion might originate from pieces of the sample that was just below the slag surface and may not be indicative of the actual corrosion of the whole sample.

If the slag surface forces can cause an increase in corrosion, then the same can be concluded for the gas bubbles that travel along the sample. The gas that is released in the coal slag travels upward through the slag along the sample. While the gas bubble travels along the sample, it's the interfaces also move along the sample possibly enhancing the corrosion. Consequently, in the case of the coal slag, due to the gas bubbles, there may be enhanced corrosion all along the sample.

In addition, those two uneven corrosion features might also act together to give larger corrosion rates. As the slag overflows and its level keeps lowering during the reaction period, different parts of the sample are exposed to this severe corrosion associated with the surface. As a result, a larger part of the sample will show enhanced degradation. Uneven corrosion problems can be avoided by using larger crucibles. A large crucible may prevent slag from overflowing, and the slag surface would stay at the same level. The behavior of both sample and slags was tested in 50mL crucibles. Figure 4-47- Sapphire in coal slag at 1400^{o}C for 4 days in 50mL crucible represents sapphire in coal slag at 1400 for 4 days (the most severe condition). There were no bubbles in the slag, and no spalling of the sample was observed.

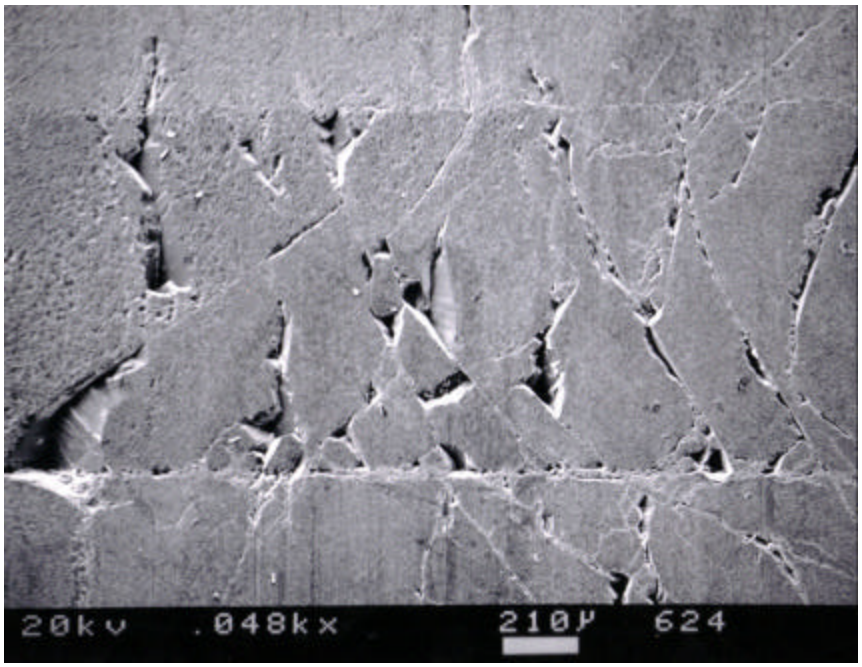

Figure 4-47- Sapphire in coal slag at 1400°C for 4 days in 50mL crucible

Since the corrosion rates are so small, and the data values vary around the zero, this variation is probably due to experimental and measurement errors. Taking for example corrosion of sapphire in coal slag at 1200°C and 1300°C, obtained data points for each temperature and time period are very similar from each other Table 4-1, but do not follow any apparent trends.

Table 4-5- Corrosion measurements of sapphire in coal slag at 1200°C and 1300°C

Days in furnace	*1200°C (mm)*	*1300°C (mm)*
1	-0.01	0.01
2	-0.01	-0.01
3	0	-0.02
4	0.01	-0.01

The clustering of data points around zero and very small corrosion rates compared to the size of measurement errors indicate that the variation is purely due to error. In fact, there is almost no corrosion taking place in this case and the plot lines are practically horizontal, as shown in Figure 4-48- Corrosion of sapphire in coal slag at 1300oC and Figure 4-49- Corrosion of sapphire in coal slag at 1200oC.

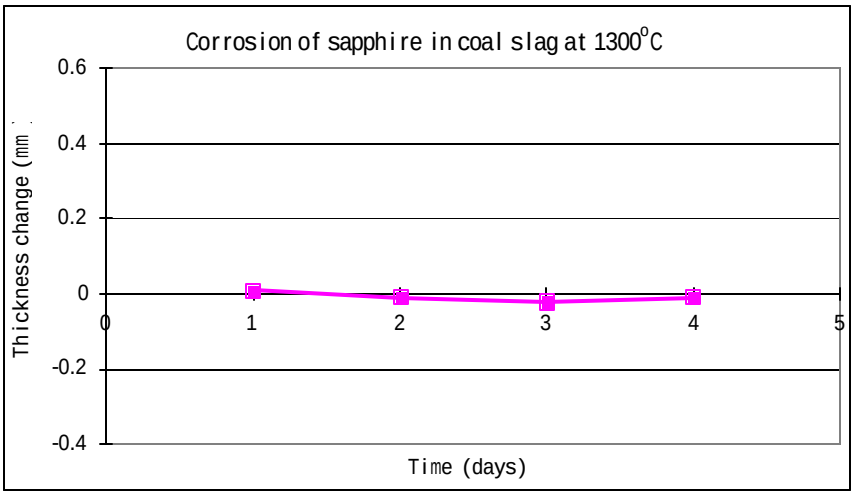

Figure 4-48- Corrosion of sapphire in coal slag at 1300°C

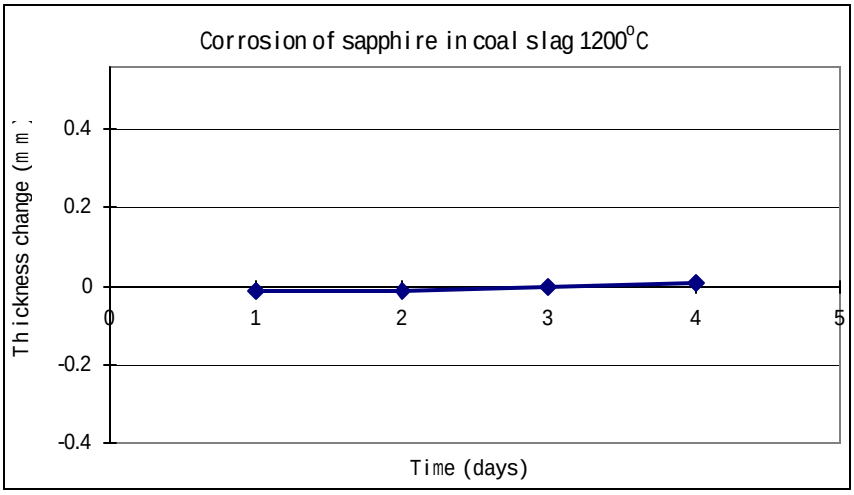

Figure 4-49- Corrosion of sapphire in coal slag at 1200°C

4.4.4 Zirconia cracking

Possible causes for cracking of zirconia samples are yttria depletion from zirconia, phase transformation from tetragonal to monoclinic and grain growth. After the yttria stabilizing agent was depleted from zirconia, zirconia underwent phase transformation from cubic to tetragonal, and then from tetragonal to monoclinic. The tetragonal to monoclinic is a rapid process accompanied with 3-5% volume expansion[28]. This volume expansion is responsible for intense cracking. The crystal structures of cubic, tetragonal and monoclinic phases are shown in.

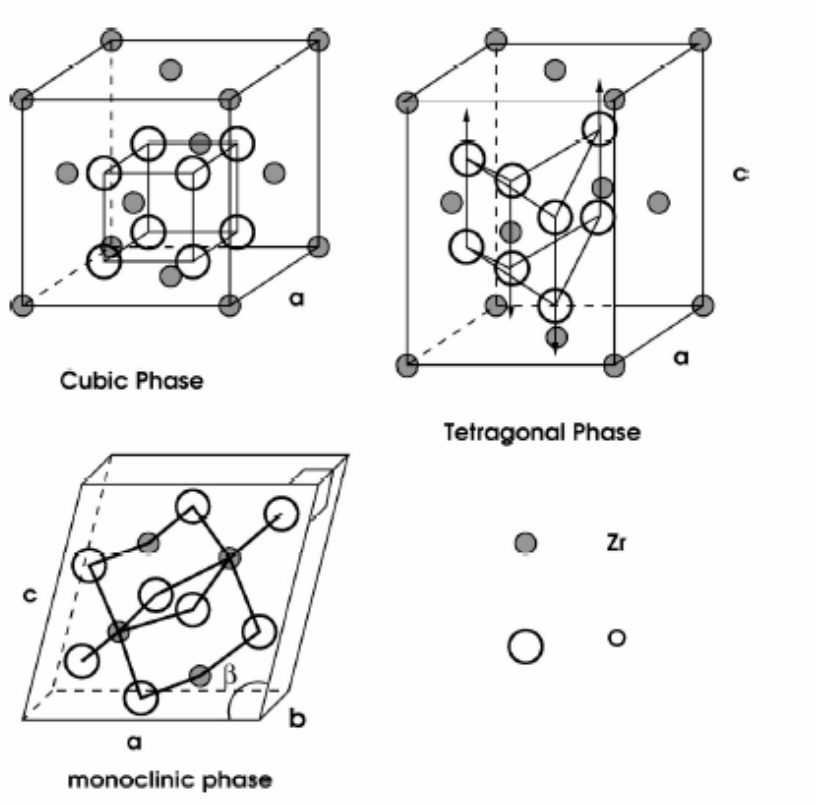

Figure 4-50- Structures of the three ZrO2 phases. The Zr-O bonds are only shown in the monoclinic structure. For the tetragonal phase, the arrows indicate the distortion of oxygen pairs relative to the cubic structure.

5. SUMMARY AND CONCLUSIONS

The extent of corrosion of single crystal sapphire and single crystal fully stabilized zirconia were investigated in severely corrosive environments such as in coal slag and soda lime glass under high temperatures. Samples of single crystal sapphire and zirconia underwent heat treatments for temperatures of 1200°C, 1300°C, and 1400°C for time periods of 1, 2, 3, and 4 days. The difference between the initial and final thicknesses of the samples represented the amount of corrosion. After the heat treatments, the slag or glass was removed by dissolving it with concentrated hydrofluoric acid. Then, the samples of sapphire and zirconia were cleaned and measured. Some difficulties in measurement were observed with zirconia. Zirconia samples would break into very small pieces during the corrosion experiments and thickness measurements were not possible. This is suspected to be due to phase change in zirconia from tetragonal to monoclinic. The phase transformation from tetragonal to monoclinic is accompanied by 3-5% volume change, which caused zirconia to crack. The obvious changes in zirconia samples were noticed as well- initially, zirconia samples were transparent while after the corrosion experiments they were opaque.

The cross section of the samples of single crystal sapphire and zirconia were examined for possibility of formation of the interfacial product or penetration of slag or glass into the sample. The SEM micrographs display no indication of existence of interfacial product. However, they reveal the intense cracking of zirconia in coal slag, and spalling of many sapphire and zirconia samples. The EDX elemental scans present clear interfaces and no sign of penetration of slag or glass constituents into the sapphire and zirconia

samples. Sapphire in coal slag exhibited an interesting phenomenon that was observed in EDX scans- separation of iron from the silicon in the slag, and its segregation to the surface (interface or gas bubbles surface).

The data indicates that there is very little or no corrosion taking place in the case of sapphire in coal slag and soda lime glass. When zirconia was corroded in coal slag and soda lime glass, it was difficult to obtain many measurable pieces of the sample due to intense cracking. For this reason, there are not many data points obtained for zirconia, but SEM and EDX analyses indicate that there is no formation of the interfacial product no penetration of slag components into the sample.

6. FUTURE WORK

The results of this work show that the corrosion resistance of sapphire as well as its attractive optical properties makes it a suitable candidate material for use in the temperature probe for coal gasifiers. Around July of 2004, the BPDI system will be installed in the coal gasifier in the Wabash River power plant facility and field tested.

The unusual remark of the iron separation in coal slag and its segregation to the interface of the sample would be interesting to further investigate. The study should explore the conditions under which the iron deposits on the sapphire surface and whether this iron coating has a diminishing effect on corrosion. This study can be conducted by researching the corrosion rates of sapphire coated with iron and the diffusion rates of the slag constituents through the iron layer. If this layer of iron has a desirable influence on corrosion of sapphire, then the sapphire can be coated with iron in order to minimize the corrosion.

REFERENCES

[1] http://www.fe.doe.gov/programs/powersystems/gasification/

[2] http://www.lanl.gov/projects/cctc/factsheets/tampa/tampaedemo.html

[3] G. R. Pickrell "High Temperature Alkali Corrosion of Low Expansion Ceramics" Dissertation, Virginia Tech (1994)

[4] Gary Pickrell, Yibing Zhang, Zorana Dicic and Anbo Wang, 20th Pittsburg Coal Conference, Pittsburgh, Pa, September, 2003

[5] Y. Zhang, G.Pickrell, B. Qi, R. G. May, A. Wang, WHAT JOURNAL?? WHEN??

[6] http://www.crystalsystems.com/sapprop.html

[7] http://www.saphikon.com/semiprop.htm

[8] http://www.crystalsystems.com/sapprop.html

[9] T. Oh, L. N. Shen, R. W. Ure, Jr. and I. B. Culter, *Engineering Note*, **56** [7] (1977) pp. 649-650

[10] T. Oh "Slag Penetration into Oxide Refractories", Masters Thesis, University of Utah, March 1997

[11] A. R. Cooper Jr. and W. D. Kingery "Dissolution in ceramics systems: I, Molecular diffusion, natural convection, and forced convection studies of sapphire dissolution in calcium aluminum silicate," *J. Am. Ceram. Soc.*, **47** [1] (1964), pp. 37-43

[12] B. N. Samaddar, W. D. Kingery, and A. R. Cooper Jr. "Dissolution in ceramics systems: II, Dissolution of Alumina, Mullite, Anorthite, and Silica in a Calcium-Aluminum-Silicate Slag," *J. Am. Ceram. Soc.*, **47** [5] (1964), pp. 249-254

[13] M. K. Ferber, V.J.Tennery, ORNL/TM-8385, October 1982

[14] http://www.azom.com/details.asp?ArticleID=133

[15] P.C. Rivas, M.C. Caracoche, A.F. Pasquevich, J.A. Martinez, A.M. Rodriguer, A.R.L. Garcia and S.R. Mintzer. *J. Am. Ceram. Soc.* **79** [4] (1996), pp. 831–836.

[16] http://cyberbuzz.gatech.edu/asm_tms/phase_diagrams/pd/y2o3-zro2.gif

[17] http://www.azom.com/details.asp?ArticleID=940

[18] T. Sato and M. Shimada. *J. Am. Ceram. Soc.* **68** [6] (1985), pp. 356–359.

[19] . Sato, S. Ohtaki and M. Shimada. *J. Mater. Sci.* **20** (1985), pp. 1466–1470.

[20] Q. Fang, P. S. Sidky, M. G. Hocking *Wear* **233-235** (1999), pp. 615-622

[21] M. Yoshimure, T. Hiuga and S. Somiya. *J. Am. Ceram. Soc.* **69** [7] (1986), pp. 583–584.

[22] Nishida A., Terai K., *Journal of Ceramic Society of Japan* **100** (1992), pp 1097-1100

[23] Derek D Hass, "Thermal Barrier Coatings Via Directed Vapor Deposition", Dissertation, University of Virginia (http://www.ipm.virginia.edu/research/PVD/Pubs/thesis6/Hass_PHD2000.pdf)

[24] http://www.hooverprecision.com/html/alumina_oxide.html

[25] V. K. Pavlovkii, Yu. S. Sobolev, "Refractory- Oxide Corrosion in Molten High-Lead Silicate Glasses" *Steklo i Keramika*, No. 6 (1991), pp. 233-236

[26] Y. D. Chang and M. E. Schlesinger *J. Am. Ceram. Soc.* **77** [3] (1994), pp. 611–616.

[27] http://www.shodor.org/UNChem/advanced/kin/arrhenius.html

[28] http://www.accuratus.com/zirc.html

VITA

Zorana Dicic, daughter of Jasminka and Ilija Dicic, was born in Belgrade, Yugoslavia (now called Serbia and Montenegro) on September 23rd 1978. She attended IX Belgrade gymnasium, Mihailo Petrovic Alas, science orientation. She graduated from Manhattan College with a B.S. degree in chemistry in May of 2001.

Zorana enrolled in a graduate program in Materials Science and Engineering department at Virginia Tech in August 2001. This thesis completes her M.S degree.